Fisheries Research
September 2016, Volume 181 Pages 198-213
http://dx.doi.org/10.1016/j.fishres.2016.03.023
http://archimer.ifremer.fr/doc/00333/44430/

Adult-mediated connectivity affects inferences on population dynamics and stock assessment of nursery-dependent fish populations

Archambault Benoit [1, 2], Le Pape Olivier [1], Baulier Loic [1, 3], Vermard Youen [4, 5], Véron Matthieu [1], Rivot Etienne [1, *]

[1] Agrocampus Ouest, UMR 985 ESE Ecologie et Santé des Écosystèmes, Rennes, France
[2] AgroParisTech, Paris, France
[3] Ifremer, Délégation de Guyane, Cayenne, France
[4] Ifremer, Channel and North Sea Fisheries Department,Boulogne Sur Mer, France
[5] Ifremer, Department of Fisheries Ecology and Modelling, Nantes, France

* Corresponding author : Etienne Rivot, email address : etienne.rivot@agrocampus-ouest.fr

benarcha@gmail.com ; Olivier.Le.Pape@agrocampus-ouest.fr ; loic.baulier@ifremer.fr ; youen.vermard@ifremer.fr ; matthieu.veron@agrocampus-ouest.fr

Abstract :

We explore how alternative hypotheses on the degree of mixing among local subpopulations affect statistical inferences on the dynamics and stock assessment of a harvested flatfish population, namely, the common sole population in the Eastern Channel (ICES area VIId). The current paradigm considers a single, well-mixed, spatially homogeneous population with juveniles from all coastal nursery grounds along the French and UK coasts that contribute to a single adult population and one pool of eggs. Based on the available data and ecological knowledge, we developed a spatial Bayesian integrated life-cycle model that consists of three subpopulations (one near the UK coast and two near the French coast, denoted UK, West FR and East FR, respectively) supported by their respective local nurseries, with the connectivity among the three components limited to low exchanges during larval drift. Considering the population dynamics among three subpopulations (instead of a single homogeneous one) drastically changes our inferences on the productivity of nursery sectors and their relative contribution to total recruitment. Estimates of the East FR subpopulation's contribution to total recruitment increase (29% in the single population model; 48% in the three subpopulation model), balanced by a decrease in the UK subpopulation's contribution (53%; 34%). Whereas an assessment based on the hypothesis of a single spatially homogeneous population in the EC indicates exploitation far above MSY (current F/FMSY = 1.8), an assessment that considers a metapopulation with three loosely connected subpopulations revealed a different status, with the UK and East FR subpopulations being exploited above MSY (current F/FMSY = 1.9 and 2, respectively) and the West FR subpopulation approaching full exploitation (current F/FMSY = 1.05). This approach contributes to the quantitative assessment of spatial fishery and coastal habitat management plans.

Keywords : Solea solea, Spatial life-cycle model, Coastal nurseries, Connectivity, Stock assessment, Hierarchical bayesian model

1. Introduction

Integrated life-cycle modeling approaches that account for the spatial structure of populations are needed to improve our understanding of the impacts of multiple pressures on populations (Carson et al., 2011; Stelzenmuller et al., 2011; Wolfshaar et al., 2011; Petitgas et al. 2013). The concepts of metapopulation were introduced long ago in the optimal harvesting theory for fisheries (Tuck and Possingham, 1994 and references therein; Hilborn and Walters, 1992). Spatially explicit models can help decision making in spatial management plans either to adapt fisheries management to local productivities (Carruthers et al., 2011; Ying et al., 2011; Guan et al., 2013) or to design networks for marine protected areas (Botsford et al., 2009; Gaines et al., 2010; Grüss et al., 2011).

However, the current paradigm in population dynamics for the assessment of the most exploited marine stocks continues to ignore metapopulation structure. One often assumes a fish stock as a single, well-mixed and spatially homogeneous population that produces a single larval pool that undergoes extensive dispersal and massive export covering the population's entire distribution area. When it is addressed at all, the question of connectivity and population structure is mostly focused on early life stages (Petitgas et al., 2013; Frisk et al., 2014), with a large body of studies designed to evaluate the influence of physical and biological processes on the survival and dispersion of eggs and larvae (Miller, 2007; Savina et al., 2010; Hinrichsen et al., 2011; Peck and Hufnagl, 2012) that govern the variability of recruitment in space and time (Chambers and Trippel, 1997; Gallego et al., 2012). The importance of larval retention in marine populations has also been emphasized (Cowen et al., 2000; Warner and Cowen, 2002), because populations that display strong retention may be locally more vulnerable to local recruitment overfishing or depletion caused by catastrophic events (Strathmann et al., 2002). However, although adult-mediated connectivity is suspected to play a major role in population functioning, much less attention has been paid to its role (Frisk et al., 2014). The movements of adults may determine the structure and dynamics of metapopulations (Stelzenmuller et al., 2011; Cianelli et al., 2013), especially when larval and juvenile retention occurs (Grosberg and Levitan, 1992), thus indicating the need for population models that account for spatial structure and connectivity at all stages (Petitgas et al., 2013; Frisk et al., 2014).

New challenges arise when building and parameterizing population models that account for the spatial structure along the life cycle: (*i*) Long spatial data series of catches, abundance indices and fishing effort are rarely available; (*ii*) Coupling oceanographic circulation models and larval individual-based models provides a way to explore larval dispersal, but larval stages are rarely accessible to observation and the validation of those models remains an open question (Miller 2007); and (*iii*) Movements in the adult stage are difficult to quantify. Mark-recapture data (Drouineau et al., 2010; Carruthers et al., 2011), natural markers and genetic studies (Hellberg et al., 2002) are costly and sometimes fail to reveal the metapopulation structure (Ward et al., 1994; Smedbol et al., 2002; Rolland et al., 2007).

It thus remains a methodological challenge to embed spatial life-cycle models within a statistical approach to derive inferences on key parameters (Planque et al., 2011). The Hierarchical Bayesian modeling (HBM) framework has proven successful for embedding complex demographic processes with various sources of noisy and incomplete data on various spatial and temporal scales (Clark, 2005; Buckland et al., 2007; Parent and Rivot, 2013); thus it can help address some of these challenges. HBM has been successfully applied to build fish population dynamic models that assimilate various sources of field surveys (Rivot et al., 2004; Massiot-Granier et al., 2014), integrate mark-recapture data to capture the spatial structure of populations (Cunningham et al., 2007; Taylor et al., 2011), and incorporate complex interactions with environmental drivers of recruitment (Ruiz et al., 2009; Rochette et al., 2013).

In this paper, using the common sole (*Solea solea*) population in the Eastern Channel (EC; ICES area VIId; Fig. 1a) as a case study, we investigate how considering alternative hypotheses about adult-mediated connectivity can affect statistical inferences on population dynamics and stock assessment. The common sole is a coastal and estuarine nursery-dependent flatfish species (Le Pape et al., 2003a; Gibson, 2004). Its population in the EC is exploited, with annual landings of approximately 4,000t. The sole's life cycle in the EC is well described (Rochette et al., 2013 and references therein): adults reproduce in early spring; pelagic eggs and larvae drift and survivors will eventually settle and metamorphose into benthic juveniles in late spring in a restricted nursery in which they grow for 2 years (Riou et al., 2001; Rochette et al., 2010). Afterwards, the fish move to wider and deeper adult areas, where their migrations remain limited (Burt and Millner, 2008).

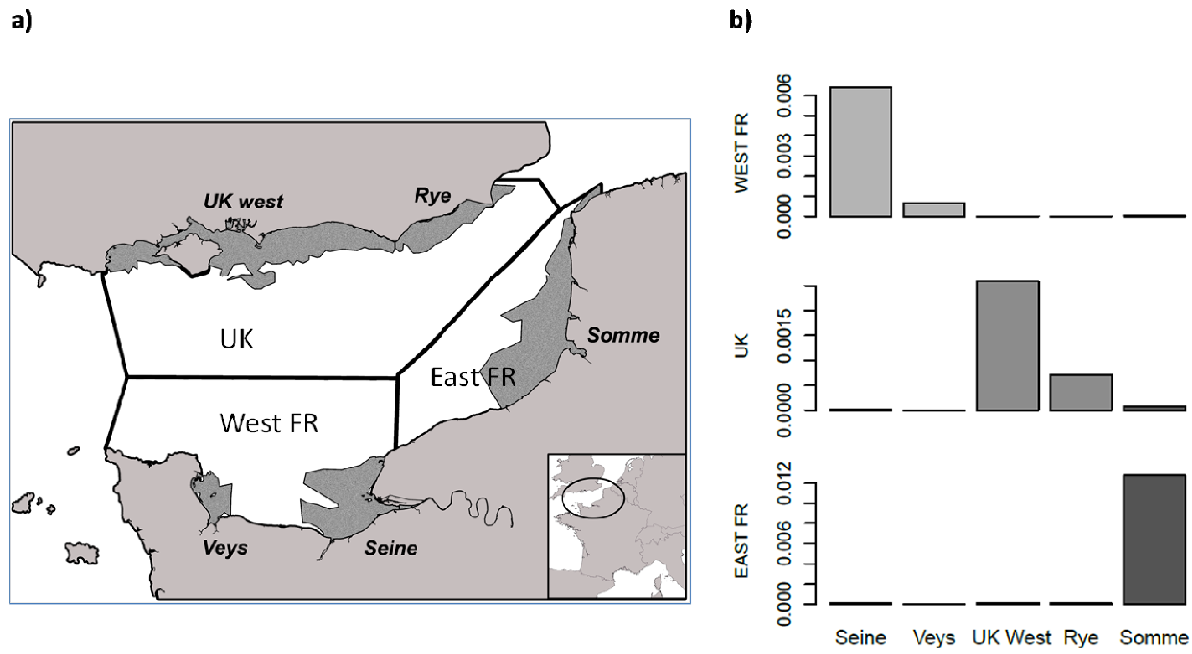

Figure 1. (a) Eastern Channel area with the spatial limits of the three subpopulations associated with the coastal nursery sectors, based on larval retention as suggested by results of the larval drift model. 1: West Fr (Veys, Seine); 2: UK (UK West, Rye); 3: East Fr (Somme). (b) Probability of successful settlement in one of the three nursery grounds (in column) given the origin of the eggs (three subpopulations as rows).

Rochette et al. (2013) have proposed an integrated life-cycle model for the EC's sole population that combines approaches that are usually considered independently: (*i*) Outputs of an individual-based model for larval drift that provided yearly estimates of the dispersion and mortality of eggs and larvae from spawning grounds to settlement in several coastal nurseries; (*ii*) A habitat suitability model based on juvenile trawl surveys combined with habitat maps to estimate the surface of each nursery sector and juvenile densities; and (*iii*) A statistical catch-at-age model for estimation of numbers-at-age and the fishing mortality of subadults and adults. A strong assumption in Rochette et al. (2013) considers that various nurseries contribute to the recruitment of a single homogeneous population in the EC. This hypothesis is consistent with the stock-assessment model (ICES, 2013). However, results from the larval drift model (Rochette et al., 2012) suggest consistent larval retention areas with strong relationships between spawning areas and nursery sectors. Additionally, ancillary data and expertise suggest only very low displacement of juveniles on nurseries (Coggan and Dando, 1988; Anon., 1989; Riou et al., 2001; Le Pape and Cognez, 2016) and only moderate movements of adults (Kotthaus, 1963; Anon., 1965; Burt and Millner, 2008) that would result in a low adult-mediated connectivity (Frisk et al., 2014). Thus, there is a strong presumption that very low connectivity exists among the three isolated subpopulations associated with different nurseries sectors, thus fostering an exploration of the impact of considering various spatial structures on (meta)population dynamics.

In this paper, we elaborate on the HBM framework proposed by Rochette et al. (2013) to explore how considering three (quasi)isolated subpopulations instead of a single homogeneous one (as considered by ICES (2013) and Rochette et al. (2013)) can affect statistical inferences on population dynamics. In particular, we assess how considering three subpopulations of adults (instead of a single homogeneous one) can change our evaluation of the productivity of each nursery area and its contributions to recruitment. We point out how consideration of three adult subpopulations ultimately affects not only the estimation of management reference points but also the assessment of the stock status with respect to the fishery's spatial dynamics.

2. Materials and methods

We first describe the model considering three (quasi)isolated subpopulations of sole in the EC (Fig. 2a), together with the available data and other model inputs based on results from previous models (Table 1). The second model that assumes a single, homogeneous adult population is derived as a simplification of the first model (Fig. 2b). Third, we provide details of the simulation method used to derive management reference points.

The life-cycle model is written in a state-space form (hierarchical) that integrates stochasticity in both the process equations for the population dynamics (process errors) and the observation equations (observation errors). All of the model equations, priors and values on fixed parameters are fully detailed in Appendix A. Posterior distributions were approximated via Monte Carlo Markov Chain methods using JAGS software (see Sup. Mat. S1 for details about the MCMC simulations and the convergence diagnostics).

Table 1. Synthesis of data and results of previous models used as inputs for the integrated life-cycle model.

		Nature of the information used	Source	Time series
EGGS & LARVAE	Survival and allocation from spawning areas to the five nursery sectors	Outputs of biophysical IBM model	Upgraded run of Rochette et al. (2012); Savina et al., in press.	1982-2007
JUVENILES	Abundance indices available for each nursery sector			
	West UK	Outputs of a habitat suitability model	Rochette et al. (2010)	1982-1999
	Rye	//	Rochette et al. (2010)	1982-2006
	Somme	//	Rochette et al. (2010)	1982-1983; 1987-2011
	Seine	//	Rochette et al. (2010) + GIP Seine Aval	1995-2002; 2006; 2008-2011
	Veys	//	Rochette et al. (2010)	2006;2010-2011
ADULTS	Available on the scale of the Eastern Channel			
	Catches at age	Data	ICES	1982-2011
	UK commercial CPUE (UKCBT)	Data	ICES	1986-2011
	Belgium commercial CPUE (BECBT)	Data	ICES	1982-2011
	Available for the three subpopulations			
	Spatial repartition of catches (total weights, no age structure) among the three areas (East FR, UK, West FR)	Data	ICES (2003-2011) Y. Vermard, Pers. comm. (1982-2002)	1982-2011
	Spatial Scientific Abundance Index (UKBTS)	Data	Y. Vermard, Pers. comm.	1990-2004; 2006-2011

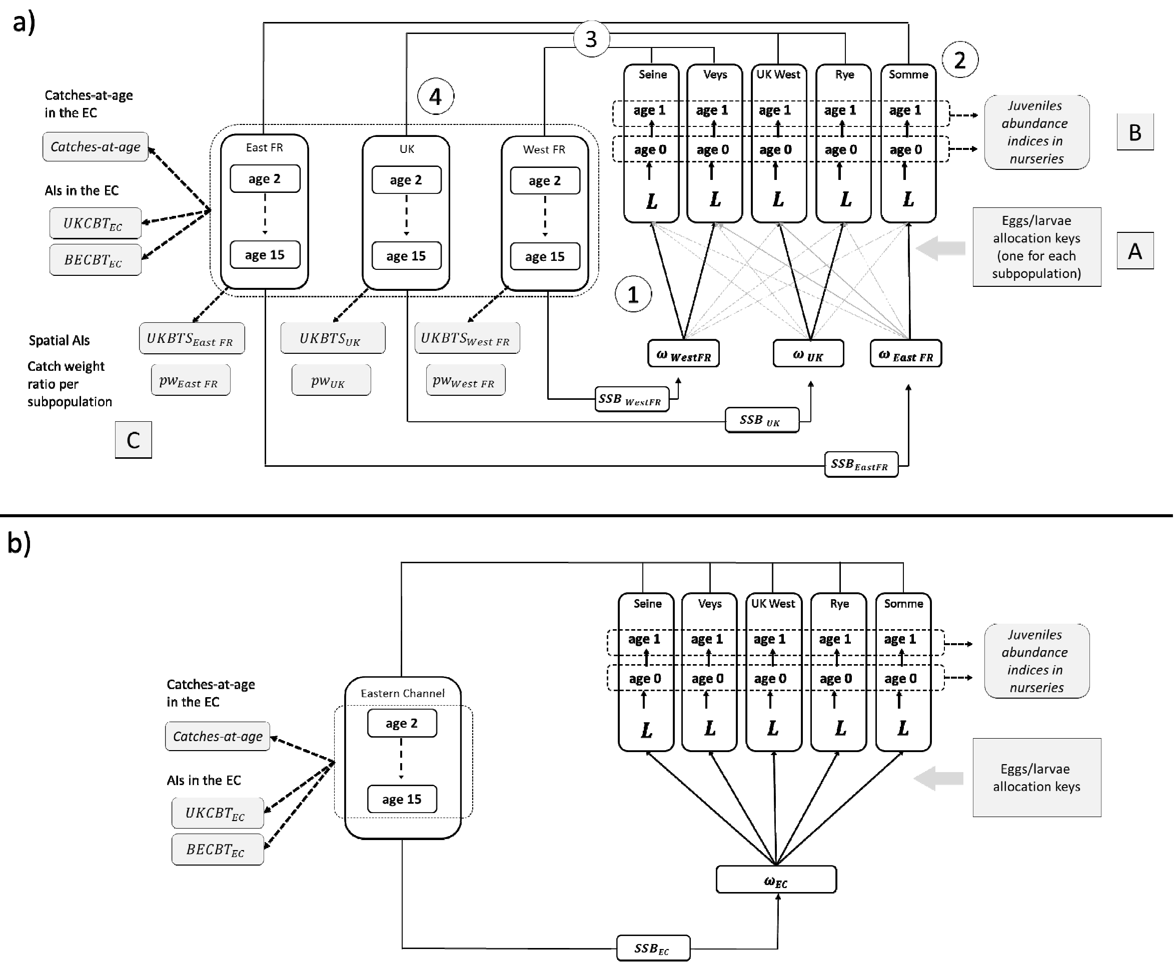

Figure 2. Hierarchical Bayesian Models for the life cycle. (a) Model with three isolated subpopulations in which only very limited mixing occurs through egg and larval drift; (b) Model considering a single population. Lettering and numbering refer to corresponding points in the *Materials & Methods* section. White boxes: non-observed state variables; Shaded boxes: data or external model outputs considered as data. Dashed arrows indicate observation equations to link latent state variables to observations.

2.1. Model considering three quasi-isolated populations

2.1.1. Spatial structure

The EC population is supported by five nursery areas (Rochette et al., 2010) along the French (Veys, Seine and Somme nurseries) and UK coasts (UK West and Rye nurseries) (Fig. 1a). Rochette et al. (2012) demonstrate the low dispersion of eggs and larvae during the pelagic stages of the common sole (Fig. 1b). Indications of the reduced movements of juveniles and adults suggest that connectivity is almost null for juveniles and only very limited for adults. Considering this limited connectivity along the life cycle and the presence of natural barriers (e.g., rocky shores in the central southern coast and deep gravel grounds in the central part of the EC; Rochette et al., 2010), three subpopulations associated with three spawning areas (denoted r=1,2,3) and attached nursery sectors were identified (Fig. 1a): the Western French subpopulation (West FR; Seine and Veys nursery sectors), the UK subpopulation (UK West and Rye nursery sectors) and the Eastern French subpopulation (East FR; Somme nursery sector).

2.1.2. Population dynamics

The population dynamics were modeled for 30 years from 1982 to 2011. The model is stage-structured from eggs to settled larvae and then age-structured from juveniles to adults (Fig. 2a).

Eggs and larvae (see 1 in Fig. 2a)

Egg hatching is parameterized following the characteristics of the spawning season and the spatial distribution of eggs (Rochette et al., 2012), and the annual quantity of eggs spawned in each of the three subpopulations directly depends on the spawning biomass. Eggs and larvae are transported from spawning areas and settle in the five identified nursery sectors according to a drift/survival matrix estimated from a biophysical model (Rochette et al. (2012). Outputs from the larval-drift model (Rochette et al., 2012; Fig. 1b) indicate very low connectivity between the three spawning areas and distant nursery sectors over the time series, each spawning area almost exclusively feeding the closest coastal and estuarine nursery grounds. Only very limited mixing of individuals between the three subpopulations then occurs through larval drift (Fig. 2a). The UK—and in lesser proportions the East FR—subpopulations were also subject to larval inputs from the North Sea's (NS) sole population (Savina et al., in press), which were integrated into the model as a constant term (not shown in Fig. 2).

Juvenile from age 0 to age 2 (see 2 in Fig. 2a)

Because of competition for space and food resources (Iles and Beverton, 2000; Le Pape and Bonhommeau, 2015), settled larvae experience density-dependent post-settlement mortality over nursery sectors between settlement (late spring) and the end of summer (growth period).

Following previous modeling work in Rochette et al. (2013) and Archambault et al. (2014), the resulting expected number of age-0 juveniles is modeled through a compensatory density-dependent Beverton-Holt (BH) relationship parameterized with local parameters α_i, the maximum survival rate (i.e., the survival rate without density dependence) and K_i, the carrying capacity per unit of surface (i.e., the maximum number of age-0 juveniles that can survive per unit of surface), which is then scaled to the total surface of each nursery, S_i (fixed). Unexplained random variations are captured by independent lognormal random noise.

Because only limited information is available to estimate site-specific parameters, exchangeable hierarchical structures (Gelman et al., 2004) were used to model the between-nursery variability of parameters α_i and K_i, enabling "borrowing strength" between nursery sectors (Rivot and Prévost, 2002; McAllister et al., 2004). Available juvenile abundance indices on nursery sectors may contain enough information to estimate the carrying capacity parameters K_i. However, because very few observations are available at low levels of settling larvae, the maximum survival rates α_i could be difficult to estimate. Informative priors were set on the α_i (see Appendix A) based on a meta-analysis of flatfish stock-recruitment relationships (Archambault et al. 2014).

Late age-0 juveniles (in September, after the summer growth period) experience a fixed natural mortality during 4 months until they reach age 1 in January. Age-1 juveniles spend one year in nursery grounds with both natural (fixed) and fishing (estimated) mortalities.

From nurseries to sub-adults (see 3 in Fig. 2a)

Young fish are assumed to leave their nurseries at age 2, in January. No quantitative data were directly available on the connectivity from nursery sectors to deeper areas where older fish live (ages 2-15). Therefore, age-2 fish leaving nurseries are supposed to contribute directly to the subpopulation adjacent to the nursery (Fig. 1a).

Sub-adults and adults (see 4 in Fig. 2a)

Fish from ages 2-15 are structured in three different subpopulations, with cohort dynamics accounting for both natural (age-specific, fixed) and fishing (age-/ year-/ subpopulation-specific, estimated) mortalities. All of the remaining fish are then assumed to die at age 15. Because the cumulative natural mortality up to age 12 is near 1, including an age+ group in the model would not change the results. Fishing mortality is a function of fishing effort (estimated) and age-specific gear selectivity (estimated).

Fish between the age of 3 and 15 participate in reproduction. The number of eggs for each year and each subpopulation is calculated from the spawning stock biomass.

2.1.3. Integration of results of previous models, data sources and observation models

Eggs and larvae survival and allocation key (see A in Fig. 2a)

Egg and larval survival and allocation from spawning areas to the five nursery sectors over 26 years between 1982 and 2007 were available as outputs from an upgraded run of Rochette et al.'s (2012) biophysical model (Savina et al., in press). That model ultimately provided the $3 \times 5 \times 26$ probability key that eggs from each of the 3 subpopulations would reach one of the 5 different nursery sectors, accounting for inter-annual variability over the 26 years of simulation. No outputs of larval drift model were available for the last 4 years (2008-2011; Table 1). Because no particular time trend appears in the time series, the 3×5 probability key for years 2008-2011 was set equal to the average over the entire series.

Abundance indices of juveniles in each nursery sector (see B in Fig. 2a)

The abundance indices (AI) of juveniles and the total surface of each nursery sector are outputs from the habitat suitability model developed by Rochette et al. (2010) and used in Rochette et al. (2013). Juvenile (ages 0 and 1) AIs over the five nursery sectors were obtained from an upgrade of Rochette et al.'s (2010) habitat-suitability model, using updated scientific trawl survey data. They were considered as lognormal random observations of juvenile abundance accounting for gear/ age-specific catchability.

Catches-at-age (see C in Fig. 2a)

Annual catches-at-age were available from stock assessment reports only at the scale of the EC; however, they were not available separately for the three subpopulations. Catches-at-age predicted by the model for each subpopulation were then first aggregated at the scale of the EC and considered observed with lognormal errors.

Ancillary data for the catch weight ratio per subpopulation (total weight; no age structure) also exist, thus showing that higher proportions of catches are regularly realized in the East FR area (subpopulation associated with the Somme nursery sector). An additional likelihood term for the catch weight ratio per subpopulation was added to assimilate this information in the model.

Abundance indices of adults (see C in Fig. 2a)

Different AIs for adults were available at various spatial scales (EC and subpopulations). Two time series of AIs were available at the scale of the EC: the UK (UKCBT) and the Belgium (BEBCT) commercial fleet catch-per-unit effort. The scientific UK Bottom Trawl Survey (UKBTS) provided AIs at the adult stage for each of the three subpopulations. One observation equation is written for each time series of AIs, each contributing to the whole likelihood function. All of the AIs were considered as lognormal random observations of abundance at age, but with catchability parameters specific to the fleet (UKBCT, BEBCT, UKBTS) age and year.

2.1.4. Choice of priors and values of fixed parameters

Some parameters were fixed from the literature (Appendix A, Table A.1). All of the estimated parameters except for the selectivity curve parameters and the slopes of the BH relationships over nursery areas (α_i) were given weakly informative *a priori* distributions in the sense of Gelman (2004), i.e., they let the data speak while excluding unrealistic values (Appendix A).

2.2. Simplifying the model to a single, homogeneous adult population

The model considering three isolated subpopulations can easily be simplified into a single population model that corresponds to the structure of Rochette et al. (2013) and to the stock-assessment working group (ICES, 2013). This single population model assumes that the five nursery sectors contribute to one single population covering the whole EC (Fig. 2b). The distribution of eggs over the spawning area is assumed to follow the distribution observed in 1991 (Rochette et al., 2012). All other processes (e.g., juvenile dynamics) are unchanged except for the fishing mortality of adults that is now considered homogeneous at the EC scale. The same sources of data are used, but no catch weight ratios per subpopulation are considered and only the adult AIs available at the EC scale (i.e., UKCBT and BECBT) are used (Fig. 2b).

2.3. Evaluating the fit to each data sources

We conducted posterior predictive checking to evaluate the fit of the model to each data source assimilated in the model. For each data source, observed data (denoted y^{obs}) were compared to the distribution of replicated data sets (y^{pred}) simulated from their posterior predictive distribution (Gelman et al., 2004). To check that the model was able to replicate data similar to the observations, we compare synthetic statistics calculated from the observed data ($T(y^{obs})$) with statistics calculated from replicated data ($T(y^{rep})$). We calculated Bayesian *p-values* (Gelman et al., 2004), defined as the probability that the statistics calculated from the replicated data $T(y^{rep})$ are more extreme than the statistics calculated from the observed data $T(y^{obs})$:

(1) $$p\text{-}values = \Pr\left(T(y^{rep}) \geq T(y^{obs})\right)$$

We chose the standard discrepancy statistic calculated for the observed and simulated data as follows:

(2) $$T(y^{obs}) = \sum(y^{obs} - E(y))^2 \text{ and } T(y^{pred}) = \sum(y^{pred} - E(y))^2$$

where y^{obs} is an observation, y^{pred} is a simulated value in the posterior predictive distribution of the state variable y and $E(y)$ is the expected mean of y in the model (the fit of the model). y^{obs}, y^{pred} and $E(y)$ were log-transformed for all variables observed with lognormal random noise. Depending upon the data source, the sums in eq. (2) are calculated either across the entire time series of available data (for age-0 and age-1 AIs in nursery sectors and for the catch weight ratio per subpopulation) or across both time and age classes (for adults AIs and aggregated catches-at-ages). *p-values* close to 0 or 1 reveal the potential failure of the model (Gelman et al. 2004).

In addition, we assessed the contribution of the various data sources in the model, considering three loosely connected populations by examining how the final inferences change when cumulating the data sources. Three runs of the model were conducted, successively adding the various spatial data series (i.e., spatial UKBTS AIs and catch weight ratio per subpopulation; Table 2). In run (a), only spatial UKBTS AIs are introduced in the likelihood. Run (b) considers a likelihood function for the catch weight ratio per subpopulation, but does not integrate spatial UKBTS AIs. Finally, run (c) corresponds to the final model that assimilates both the spatial UKBTS AIs and the catch weight ratio per subpopulation.

Table 2. Configuration of the three model runs to explore the respective contributions of data sources to the fit of the model with three subpopulations.

Run	**Spatial Abundance Index (UKBTS)**	**Proportion of total catches among subpopulations (total catches in weight, no age structure)**
a	Yes	No
b	No	Yes
c	Yes	Yes

2.4. Stock-assessment and management reference points

The spawning stock biomass (SSB), recruitment (R), fishing mortality (F), and Maximum Sustainable Yield (MSY, the associated fishing mortality (F_{MSY}) and spawning stock biomass (SSB_{MSY}) were estimated on different scales (for each subpopulation and on the scale of the EC).

The evaluation of MSY, F_{MSY}, and SSB_{MSY} is not analytically straightforward, because the production of each subpopulation results from a combination of stochastic BH relationships fitted on each nursery sector (two in West Fr: Veys and Seine; two in the UK: UK West and Rye; and one in East FR: Somme; Fig. 1a). The empirical equilibrium curves were obtained using Monte Carlo simulations to integrate both process and parameter uncertainty (see the methods in Appendix B). In the model considering three subpopulations, reference equilibrium points for each subpopulation r, denoted $B_{MSY,r}$, $F_{MSY,r}$ and $C_{MSY,r}$, were estimated conditionally by fixing the fishing pressure for the two other subpopulations equal to the estimates averaged over the last five years of the data series (2007-2011).

3. Results

3.1. Model evaluation

For both of the model configurations, the convergence diagnostics indicate convergence of the MCMC chains after 10^6 iterations for all variables (see Sup. Mat. S1 for more details about the MCMC simulations and the convergence diagnostics). To reduce the autocorrelation in the sample used for final inferences, one out of 100 iterations was kept (thinning = 100). Final inferences were derived from a sample of $3 \times 10{,}000$ iterations that resulted from merging the three chains.

Because the two models integrate different sources of data (e.g., the spatial AIs of adults and catch weight ratios that are not included in the model considering a single, homogeneous adult population), the usual goodness of fit criteria cannot be used directly to compare the two model structures. The component of deviance associated with the data shared by the two model structures (i.e., the juvenile AIs in the five nursery sectors and the non-spatial AIs for ages 2-15) was revealed as slightly lower for the model with one single population than for the model with three isolated subpopulations (not shown). However, the difference is very low, indicating that the likelihood of the two models is quite comparable when considering the data shared by the two model structures.

Although this is not formally considered in the likelihood function, we also compared egg distribution among the three spawning areas (i.e., the function of the SSB associated with each subpopulation) to the spatial distribution of eggs given by the single available observation originating from the 1991 eggs survey (Rochette et al., 2012). Results indicate that the spatial distribution of eggs derived from the fit of the model with three isolated subpopulations (West FR, 29%; UK, 33%; East FR, 38%) was highly consistent with the egg distribution observed in 1991 (25%, 34% and 41%), thus providing evidence that the spatial repartition of the SSB inferred from the model considering three subpopulation is consistent with some external data sources.

Overall, a posterior predictive check conducted for the two model configurations (one homogeneous population and three isolated subpopulations) did not reveal any strong and general inconsistencies between the fitted model and the data. Almost all of the *p-values* are between 0.05 and 0.95 for all model compartments (Table 3). The additional figures included in Sup. Mat. S2 (Fig. S2.1- S2.9) show a good consistency between the posterior predictive distributions and the data, providing additional evidence of a lack of conflict between the different sources of observations assimilated in the model. Interestingly, the *p-values* associated with the data sources that are common to the two model configurations (juveniles AIs, aggregated catches-at-ages and commercial CPUEs) were quite similar between the two model configurations (Table 3).

Table 3. *p-values* of posterior predictive checking calculated for each source of observation and for the two model configurations: the model considering a single, homogeneous adult population and the model considering three subpopulations. *p-values* are the probability that the discrepancy static calculated for predicted values is greater than the one calculated with observed values (see text for details).

		One single population		**Three subpopulations**	
JUVENILES	AI in each nursery sector	Age-0	Age-1	Age-0	Age-1
	Solent (West UK)	0.72	0.74	0.92	0.51
	Rye	0.29	0.84	0.33	0.80
	Somme	0.12	0.26	0.23	0.11
	Seine	0.65	0.70	0.71	0.83
	Veys	0.61	0.55	0.72	0.64
ADULTS	Aggregated data (Eastern Channel)				
	Catches-at-age	0.54		0.56	
	UK commercial CPUE (UKCBT)	0.82		0.88	
	Belgium commercial CPUE (BECBT)	0.72		0.78	
	Spatial data				
	Proportion of total catches (weight) among the three areas (East FR, UK, West FR)				
	West FR	-		0.54	
	UK	-		0.57	
	East FR	-		0.47	
	Spatial Scientific AI Index (UKBTS)				
	West FR	-		0.85	
	UK	-		0.91	
	East FR	-		0.27	

There was however evidence of poor fit between the posterior predictive distribution from the model and the observed data for the abundance indices of age-0 juveniles in the Solent nursery sector in the case of a model considering three subpopulations (*p-value* = 0.92) (Fig.

S2.1). Additionally, *p-values* for commercial AIs (UKCBT and BECBT) and for the spatial AIs of adults (UKBTS) for the UK subpopulation are relatively high, indicating that the dispersion of the predictive distribution around the model fit is higher than the dispersion of observations (see also Fig. S2.1 and S2.8).

3.2. Posterior estimates of parameters

Marginal posterior distributions of all of the parameters obtained under both model configurations reveal that the parameters are generally estimated with low uncertainty (Sup. Mat. S3, Figs. S3.2 and S3.5 and Tabs. S3.1 and S3.2). Overall, the differences between the prior and the posterior reveal that the distributions are mostly driven by the data (Sup. Mat. S3, Figs. S3.2 and S3.5).

Interestingly, considering the more complex spatial structure of the population (three subpopulations of adults versus a single, homogeneous population) does not increase the posterior uncertainty about parameters. In contrast, uncertainty about posterior estimates of biomass, recruitment, and fishing mortality is higher in the model that considers three subpopulations (Fig. 3).

Nevertheless, one exception to this rule relates to the parameters for the density-dependent recruitment process in each nursery sector; those parameters are estimated with much more uncertainty than are the other parameters for both model configurations (Sup. Mat. S3, Fig. S3.1 and S3.4). Uncertainty is particularly high for the maximum survival rate α for the Somme and Rye nursery sectors. The posterior distribution of α for the Bay of Veys is not different from the posterior predictive distribution because juvenile abundance indices are only available for three years for this nursery sector.

For both model configurations, the selectivity parameters are estimated with very low uncertainty that leads to a knife-edge selectivity curve, with selectivity near 0 for age-1 fish, near 0.5 for age-2 fish and 1 for older fish.

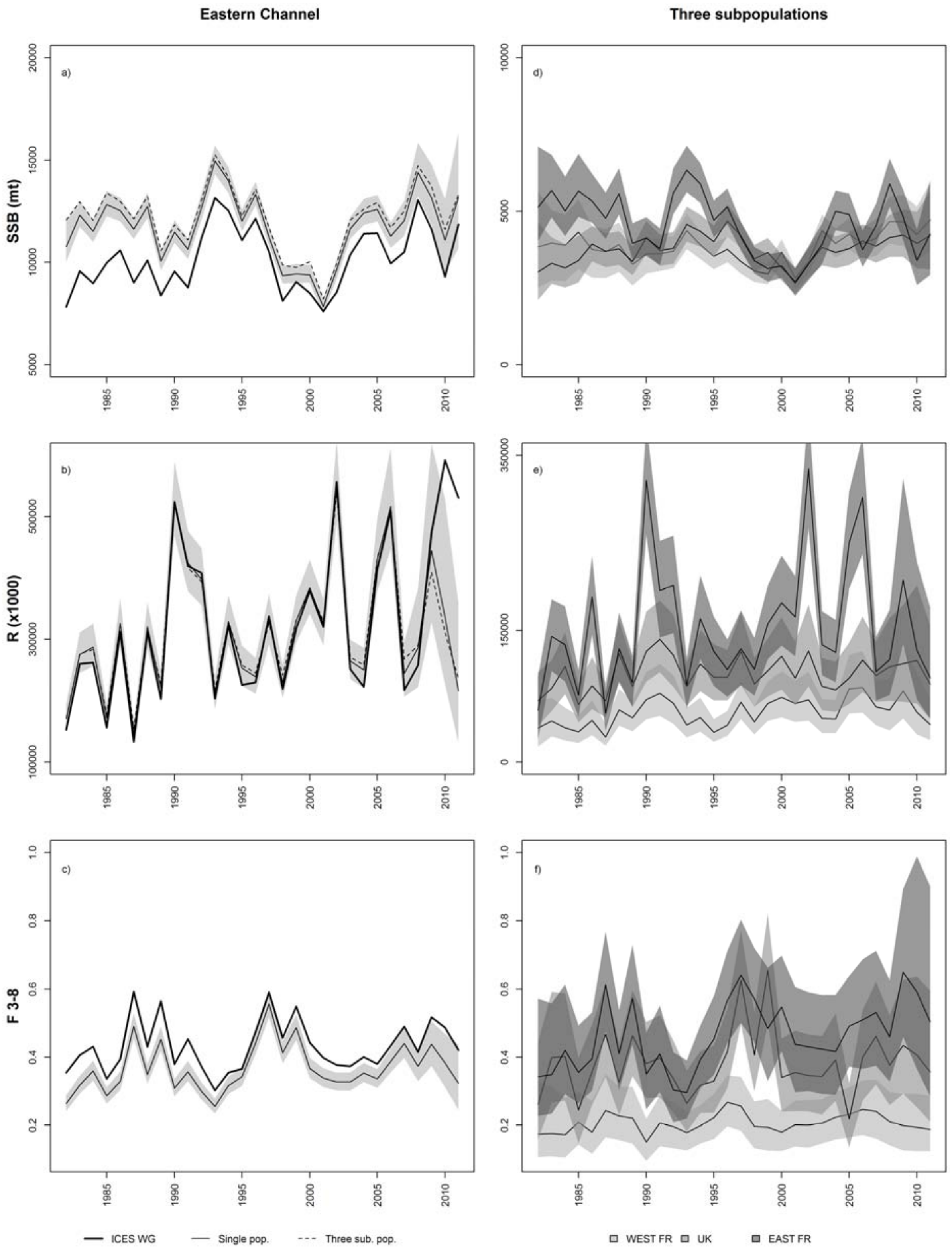

Figure 3. Left column (a, b, c). Comparison of estimates of SSB, R and F_{3-8} at the Eastern Channel scale obtained by the ICES WG (bold line) both by the model considering one homogeneous adult population (solid line) and by the model considering three components of the adult population (dotted line). Right column (d, e, f). Estimates of SSB, R and F_{3-8} for the three subpopulations. Plain lines: posterior medians. Shaded areas: 95% Bayesian credible intervals.

As expected, the process error variance of the larvae to age-0 transition is greater than for the age-0 to age-1 transition (Sup. Mat. S3, Tabs. S3.1 and S3.2). This residual variability does not reveal any particular departure from the hypotheses of constant variance across the five nursery grounds and of the time independence of residuals (not shown).

In both model configurations, the variance of observation error in catches is very low. In the model considering a single, homogeneous population, the observation error on juveniles and adults' abundance indices are of the same order of magnitude. In contrast, the variance of observation error among juveniles is much higher in the model that considers three subpopulations.

Additional results (Sup. Mat. S3, Tabs. S3.3 and S3.4) reveal that some parameters are correlated and thus partially confounded. Results are similar for the two model configurations. In particular, parameters (α,K) for each nursery sector are negatively correlated. Catchabilities associated with age-0 and age-1 abundance indices (q_0 and q_1) are positively correlated; moreover, they are positively correlated with the variance of observation errors on juveniles (σ^2_{Ijuv}). Similarly, catchabilities associated with adults' abundance indices (q_{UKCBT}, q_{BECBT} and q_{UKBTS}) are positively correlated, and they are positively correlated with the variance of observation error (σ^2_{IAd}).

3.3. Contribution of the different data sources to posterior estimates

We assessed the contribution of each dataset to the final estimations of the model with three subpopulations. Three runs of the model were conducted, successively assimilating the different sources of spatial data series (i.e., spatial UKBTS AIs and proportion of catches among areas; Table 2). The spatial AIs and the spatial distribution of aggregated catches make different contributions to the final estimates. In the run with spatial AIs only, although the uncertainty about local SSB is relatively high, the total SSB at the scale of the EC is precisely estimated (not shown) and the repartition is relatively balanced among the three subpopulations (Fig. 4a), which is consistent with the information provided by the spatial UKBTS AIs. When including spatial catches only (no spatial AIs), differences in SSB among subpopulations are higher (Fig. 4b), with higher estimates of SSB in the UK and East FR areas than in the West FR area, which is consistent with the higher proportion of catches observed in the East FR area (see Fig. S2.6 in Sup. Mat. S2). Finally, when assimilating all available data, uncertainty in SSB estimates is drastically reduced and the variability across subpopulations is shrunken (Fig. 4c) according to the information provided by the spatial AIs, and unbalanced catch ratios translate into unbalanced fishing mortality among subpopulations.

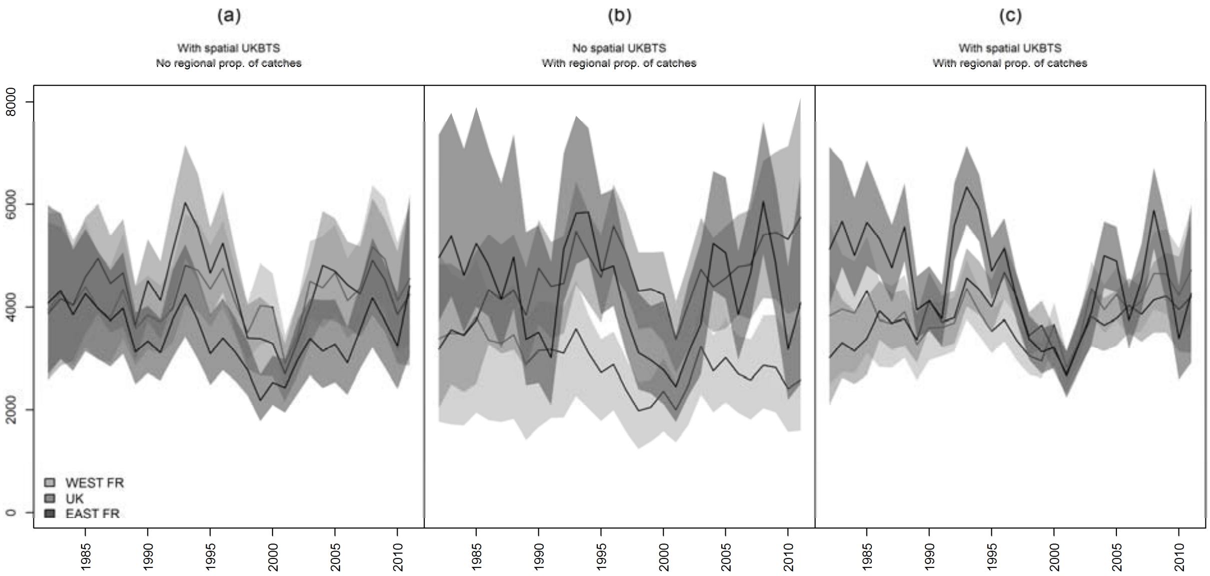

Figure 4. Time series of posterior estimates of SSB for the three subpopulations obtained with the three data configurations of the Table 2. Solid lines: posterior medians. Shaded areas: 95% Bayesian credibility intervals.

3.4. The effect of considering three isolated subpopulations on stock productivity

The effect of considering three isolated populations (instead of one homogeneous population) depends upon the spatial scale considered. The single-population model and the model considering three subpopulations provide similar estimates of SSB, recruitment and fishing mortality considered on the EC scale (Fig. 3a,b,c). These estimates were also consistent with ICES estimates, although overall they displayed a slightly higher SSB balanced by a lower F. However, the consideration of three subpopulations provides a spatial perspective on population dynamics. It also impacts inferences on stock productivity and therefore the assessment of stock status with respect to reference points.

3.4.1. Reevaluation of the productivity of nurseries

The hypothesis on the spatial structure of the population strongly affects estimates of the carrying capacity per unit of surface (Fig. 5a), with K for the Somme nursery sector being largely reevaluated when considering a model structure with three isolated subpopulations, balanced by a decrease in estimates of K for all other nursery sectors. Estimates of parameters

α for the UK West and Veys decrease when considering a model with three subpopulations, whereas the estimate increases for the Somme (Fig. 5b). Additional figures S3.3 and S3.6 in Sup. Mat. S3 provide a plot of the resulting Beverton-Holt curve in each nursery sector that illustrates the change in the local recruitment dynamics between the two model configurations.

As a result, the contributions of each nursery sector to recruitment in the EC are also strongly affected. In the single-population model, the Seine, Veys, UK West, Rye and Somme sectors contributed an average of 16, 3, 28, 24 and 29%, respectively, but with high variability among years (Fig. 6a). When considering three isolated subpopulations (Fig. 6b), these contributions were estimated at 14, 4, 17, 17 and 48% and were much less variable in time. At the subpopulation level, this translates into a strong increase in the contribution from East FR subpopulation (Somme: from 29% to 48%) balanced by decreases in contributions from West FR (Seine + Veys: from 19% to 18%) and UK subpopulations (UK West + Rye: from 52% to 34%).

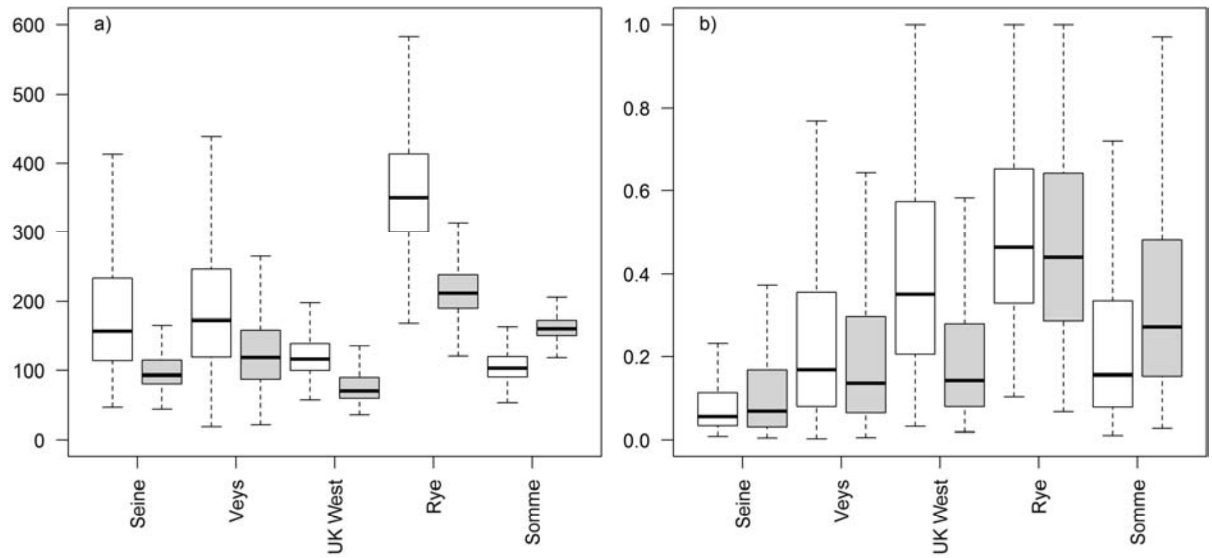

Figure 5. Marginal posterior distributions of the nursery-specific Beverton-Holt parameters K (a) and α (b) obtained with the model considering one homogeneous adult population (white) and with the model considering three isolated subpopulations (gray). K is in thousands of fish per km². α is a maximum survival rate.

Overall, those results are consistent with the high proportion of catches recorded in the East FR area (the area associated with the Somme nursery sector), logically leading to a high *SSB* in this area in the model that considers three subpopulations (Fig. 3d); in turn, this leads to higher recruitment in the Somme nursery sector.

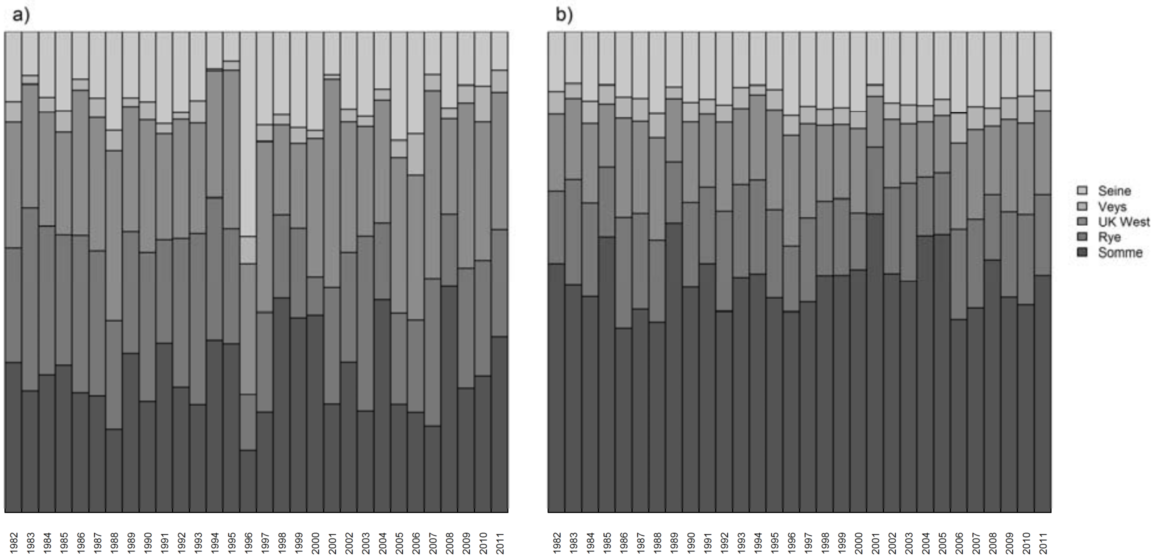

Figure 6. Contributions of the five nursery sectors to the total 0+ recruitment obtained from the model considering a) one single adult population and b) three isolated subpopulations. The contribution is calculated from the posterior median estimates of the recruitment (age-0 abundance).

3.4.2. Management reference points and stock assessment

Whereas the results obtained on the scale of the entire EC indicate that the sole population is overexploited, the results obtained when considering a three-subpopulation structure revealed highly contrasting levels of exploitation among subpopulations.

When considering a single population, the average SSB and F_{3-8} over the past four years were approximately 12,950t and 0.38, respectively (Fig. 3a,b,c). SSB_{MSY}, C_{MSY} and F_{MSY} are estimated at 28,090t, 5,470t and 0.21, respectively (Table 4; Fig. 7a), thus indicating that the sole population is currently overexploited, with an average ratio of F/F_{MSY} near 1.8 and that of SSB/SSB_{MSY} near 0.5 during the last four years.

The model with three isolated populations provides a spatial perspective on the population dynamics and the impact of fishing pressure. Estimates of SSB among the various subpopulations (Fig. 3d) are essentially equivalent, with an average SSB of 4,570t for the West FR subpopulation, 4,130t for the UK subpopulation, and 4,590t for the East FR subpopulation. By contrast, average F are highly contrasted among populations, with average F over the past 4 years estimated at 0.20, 0.39 and 0.55 for the West FR, UK and East FR subpopulations, respectively.

Table 4. Summary of point estimates of the management reference points SSB_{MSY}, C_{MSY} and F_{MSY} obtained in the models considering (i) a single population and (ii) three isolated subpopulations.

Reference points	One single population	Three subpopulations	
SSB_{MSY}	28,090	West FR	4,880
		UK	8,540
		East FR	8,300
C_{MSY}	5,470	West FR	870
		UK	1,670
		East FR	2,150
F_{MSY}	0.21	West FR	0.19
		UK	0.21
		East FR	0.28

The reference points $SSB_{MSY}, C_{MSY}, F_{MSY}$ (Table 4; Fig. 7b) associated with each subpopulation were estimated at 4,880t, 870 t and 0.19 for West FR, 8,540t, 1,670t and 0.21 for UK and 8,300t, 2,150t and 0.28 for East FR, respectively. When considering the current state of exploitation (average over four years), it appears that the West FR subpopulation is at full exploitation level, with F/F_{MSY} at 1.05 and SSB/SSB_{MSY} at 0.94, whereas the UK and East FR subpopulations are overexploited (Fig. 7b), with F/F_{MSY} dramatically greater than 1 (1.9 and 2.0, respectively) and SSB/SSB_{MSY} dramatically lower than 1 (0.48 and 0.54, respectively).

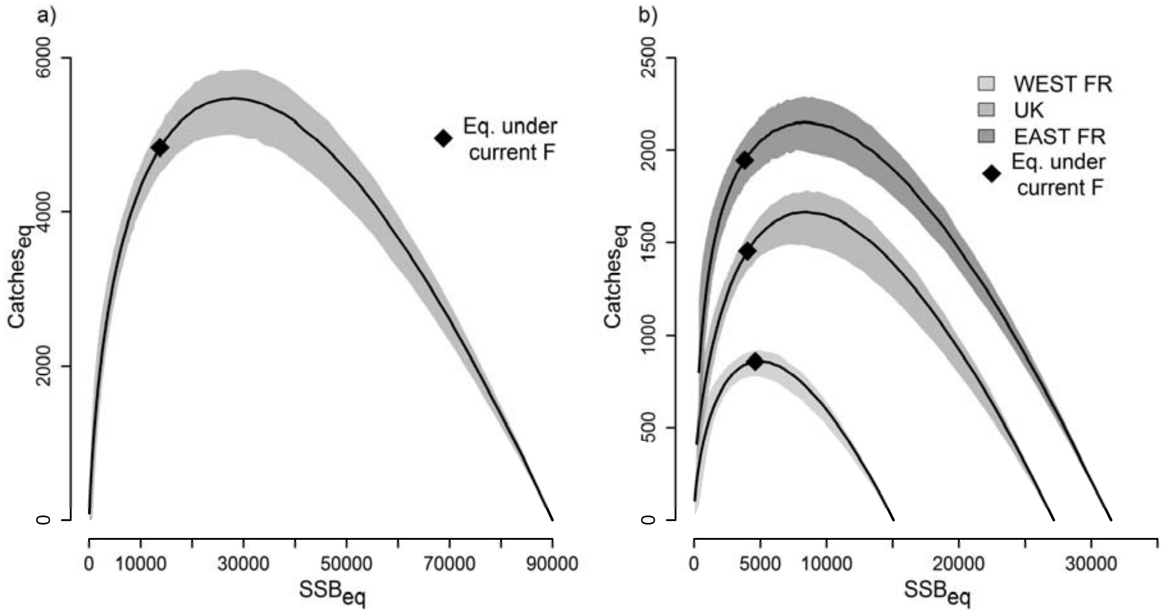

Figure 7. Relation between the SSB and catches at equilibrium obtained through the simulation approach in the model considering (a) a single population and (b) three isolated subpopulations. Shaded area: 50% credibility interval obtained from the Monte Carlo simulation integrating both process and parameters uncertainty. Black diamond: *Eq. under current F* represents the position on the equilibrium curve obtained with the current fishing mortalities (average over the 4 most recent years).

4. Discussion

4.1. An integrated modeling framework for a better understanding of metapopulation dynamics

Our results make a significant contribution to the understanding of the sole population dynamics in the EC. The model used to assess the stock of the sole population in the EC considers a simple, homogeneous population with no spatial structure (ICES, 2013). Using the HBM framework, Rochette et al. (2013) make an important contribution by establishing the fundamental basis for a population model that embeds egg and larval drift and survival derived from an oceanic circulation model within a stage-structured life cycle, accounting for the spatial nature of the recruitment process in distinct coastal nursery sectors. The model presented here elaborates on Rochette et al. (2013) and provides additional insights into population dynamics by exploring a metapopulation structure with very low connectivity among three subpopulations. The capacity of Bayesian models to incorporate prior information also presented the possibility of an efficient use of the available information through the informative prior distribution for the maximum survival rate between settled larvae and 0+ juveniles derived from a meta-analysis on flatfish (Archambault et al., 2014).

The consideration of three loosely connected subpopulations increased the model's state-space dimension of the model. But because the two models integrate different sources of data (e.g., spatial AIs of adults and catches that are not included in the model considering one single homogeneous adult population), the usual goodness-of-fit criteria such as the deviance information criterion (Spiegelhalter et al., 2014) are not adapted to compare the tradeoff between the two model structures' complexity and quality of fit. A posterior predictive check conducted for both model configurations did not reveal any strong, general inconsistencies between the fitted model and the different sources of data for both model configurations. Interestingly, when considering the data sources that are common to the two model configurations (*i.e.*, juveniles AIs, catch-at-ages and commercial CPUEs aggregated at the scale of the EC), both model configurations showed similar quality of fit. Additional results (not shown) indicate that the likelihood components restricted to the data shared by the two model structures are comparable between the two models.

However, although we were unable to demonstrate that the model considering three isolated subpopulations provides a better fit to the data, a body of ecological knowledge and clues continues to strongly argue for *a priori* consideration of such a metapopulation structure, and posterior inferences provide a portfolio of ecologically meaningful results.

First, strong prior knowledge exists in favor of the limited movements of juveniles (Coggan and Dando, 1988; Anon., 1989; Le Pape and Cognez, 2016) and adults (Kotthaus, 1963; Anon., 1965; Burt and Millner, 2008), and barriers linked to sediment structure limit exchanges between regions (Rochette et al., 2010; 2012). This knowledge was used *a priori* to define the spatial contours of three subpopulations of the common sole in the EC.

Second, taking into account the moderate connectivity between the successive life stages, we were able to produce a diagnosis of the population that, while consistent with ICES estimates at the scale of the EC, provided contrasting, meaningful results on a local scale. This approach allowed us to reconstruct local biomasses' evolution during the past three decades that were revealed as consistent with the time series of spatial abundance indices and catches. The consideration of three subpopulations also led to a substantial reevaluation of the productivity of the various nursery sectors that are quantitatively consistent with the juveniles AIs, catches and local biomasses estimated for their associated subcomponents. It also drastically reduced the between-years variability of the relative contribution of each nursery sector to total 0+ recruitment, which is consistent with both the concentration hypothesis (Rijnsdorp et al., 1992; Iles and Beverton, 2000; Rooper et al., 2004) and the low recruitment variability described for common sole (Le Pape et al., 2003b; Archambault et al., 2014).

Finally, results indicate that the spatial distribution of eggs derived from the fit of the model with three subpopulations with low connectivity matches the observed egg repartition derived from the 1991 eggs survey (Rochette et al., 2012). Because the comparison between the spatial distribution of eggs observed (1991) and simulated *a posteriori* by the model is not included in the likelihood function, this result can be considered as an element that validates the spatial structure of the adult population.

4.2. Weaknesses and directions for future research

Our modeling approach has some weaknesses. Below, we discuss some of those weaknesses along with some critical needs for knowledge and data about the spatial ecological process that the modeling approach has helped identify. Finally, we highlight a few research avenues that would improve both the knowledge and the models.

4.2.1. Simulations to explore the tradeoff between model complexity and data availability

Several studies have shown that in the case of complex spatial population dynamics, the explicit consideration of spatial structures in stock-assessment models that are better aligned with ecological reality (instead of simpler models) provide better estimates, when sufficiently informative data are available (Hulson et al., 2013; Hintzen et al., 2015). However, our case study is a data-poor situation because only a few data provide information about the spatial structure of the population. In particular, no time series of spatial catch-at-age data are available. Thus, it is difficult to formally conclude that fitting a spatial structure to the available data results in reliable estimates of abundance and population dynamics. To reinforce the analysis, one interesting perspective for future work would consist of conducting simulations that would cross a few hypotheses about how the dynamics of the true population work with various model and data configurations for the statistical stock-assessment model. This would enable us not only to show which type of assessment might provide reliable estimates given our data limitations but also to illustrate how gathering more informative data about the spatial processes (for instance spatial catch-at-age or mark-recapture data) would improve the quality of our inferences.

4.2.2. Sensitivity to priors

Uncertainty about estimates and sensitivity to the prior choice varied according to model compartment. As analyzed (with respect to a previous version of the model) by Rochette et al. (2013), numbers-at-age and all other variables associated with the demographic of ages 1-15, such as SSB, recruitment and fishing mortality, are estimated with low uncertainty. Indeed, the demographics of ages 1-15 consist of a catch-at-age model for 14 age classes tracked over 30 years; both catch and abundance indices are available for almost all years and ages.

By contrast, parameters for the density-dependent recruitment process in nursery sectors are estimated with much more uncertainty and are partly confounded. Those parameters are generally difficult to estimate from the data alone (Conn et al., 2010) and we therefore developed a method based on a previous meta-analysis on flatfish (Archambault et al., 2014) to build an informative prior distribution about the maximum survival rates of settled larvae on nursery ground (α). Relying on a previous analysis by Rochette et al. (2013), our results are likely to be sensitive to the choice of priors on those parameters, and using weakly informative priors on the α_i's would certainly lead to poor inferences about stock productivity. Because the models developed in this manuscript have many similarities and the data are the same, and to keep the main message centered on the impact of changing the spatial structure of the model, we did not report any additional sensitivity analysis.

4.2.3. Improving the model for the recruitment process

Based on previous modeling work by Rochette et al. (2013), strong hypotheses were made on the recruitment process: (i) Within each nursery sector, variability of the recruitment process was modeled as independent lognormal random noise, with no time series autocorrelation; (ii) The variance of lognormal process noise was considered homogeneous among nurseries; and (iii) Between-years random variations were considered as independent among nursery sectors. Consistent with results found by Rochette et al. (2013), a careful examination of the residual variability did not reveal any particular departure from the hypotheses of constant variance across the five nursery grounds and the time independence of residuals. This is consistent with previous analysis on the low synchronicity in inter-annual variability of juvenile abundance between the nursery sectors (Riou et al., 2001). Because there are many gaps in the time series of juvenile-abundance indices on nursery sectors (47% missing data; see Tab. 1), data are lacking to estimate parameters for the covariance in the recruitment process among nursery sectors. Including covariance in the recruitment process among nursery sectors would likely impact the population dynamics and stock assessment (Ranta et al., 1997; Liebhold et al., 2004). Therefore, an investigation of how the inclusion of covariance in the time series of recruitment process noise among nursery sectors would change estimates and population dynamics for the sole population in the EC would be an interesting focus for future research.

4.2.4. The need for better knowledge of adult-mediated connectivity

Data on sub-adult and adult migration were lacking, and we were unable to estimate the degree of mixing among the three subpopulations. Our approach thus considered two extreme scenarios of adult-mediated connectivity: full connectivity and full spatial segregation between subpopulations associated with nursery sectors. Whereas a body of ecological knowledge advocates for a loose connectivity among the three subpopulations, improved data collection on movements and connectivity is a top priority. Natural markers, which include genetic markers, xenobiotics, stable isotopes, otolith microchemistry and parasites and their possible combination (Selkoe et al., 2008; Fodrie and Herzka, 2013), are a first source of data. The analysis of genetic-neutral markers could help infer population structure (Smedbol et al., 2002), although the open nature of the marine environment may prevent a significant signal from emerging (Waples, 1998; Exadactylos et al., 2003; Rolland et al., 2007). Recent approaches using genetic-adaptive markers (Diopere et al., 2013) and combined multi-marker approaches (Cuveliers et al., 2012) provide fruitful perspectives to quantify connectivity among marine subpopulations with a finer spatial resolution. Analyses of the differences in otolith elemental composition have been used to identify the estuarine origin of individuals (Cuveliers et al., 2010). Mark-recapture is also widely used to quantify migration (Hilborn, 1990; Rijnsdorp and Pastoors, 1995; Polacheck et al., 2010). Recent work focusing on older juvenile, sub-adult and adult flatfish emphasizes the interest of these approaches (Sackett et al., 2008; Fairchild et al., 2009; Furey et al., 2013). Future methodological work should include the development of integrated models that enables the consideration of multiple sources of data into space-structured population models (Darnaude and Hunter, 2008; Korman et al., 2012; Goethel et al., 2014).

4.3. Implications for spatial management

The sole population in the EC, like most exploited marine fish stocks, is currently assessed as a single population. However, our results suggest that the consideration of metapopulation dynamics strongly impacts inferences on stock productivity and conclusions about both stock assessment and (ultimately) fisheries advice.

The consideration of three subpopulations induced a substantial reevaluation of the productivity of the various nursery sectors; estimates of the contribution of the East FR subpopulation to the total recruitment doubled, balanced by a decrease in contributions from the West FR and UK subpopulations. Whereas results obtained on the scale of the entire EC indicate that the sole population is exploited far above MSY, assessments obtained when considering a three-subpopulation structure revealed highly contrasting levels of exploitation among subpopulations, with over-exploitation of some of the metapopulation components. Indeed, estimates of local management reference points associated with each subpopulation revealed that the West FR subpopulation is approaching full exploitation, whereas the UK and East FR subpopulations are overexploited. The practical consequences of our conclusions may even increase when considering the local fisheries, which are characterized by fleets with limited movement, without large-scale tracking of fish (Tidd et al., 2015).

Beyond our case study, this work emphasizes the role of space in population functioning for species whose different life-history stages are segregated among specific habitats. Larval retention in marine populations is suspected to occur more than originally thought (Cowen et al., 2000; Warner and Cowen, 2002). Juvenile segregation in restricted nursery areas is also a common feature of fish populations (Vasconcelos et al., 2014). As noted by Frisk et al. (2014), our case study stresses the need to more thoroughly assess the importance of adult-mediated connectivity. Spatial integrated life-cycle models such as the one developed in this work provides a contribution to the quantitative assessment of spatial fishery and coastal habitat management plans. First, as previously shown by several authors, ignoring metapopulation structure in stock assessment models could result in local over/under exploitation (Tuck and Possingham, 1994; Ying et al., 2011; Yau et al., 2014) and improving data collection and statistical methods to estimate the parameters of spatial life-cycle models is a top priority for the optimal allocation of fishing pressure. Second, accounting for metapopulation dynamics is critical for an optimal assessment of essential habitat preservation and/or restoration that could be at least as efficient as assessing fishing pressure for restoring populations of nursery-dependent species (Levin and Stunz, 2005; van de Wolfshaar et al., 2011).

Acknowledgements

This work was funded partly by the European Community's Seventh Framework Programme (FP7/2007-2013) under Grant Agreement No. 266445 for the project Vectors of Change in Oceans and Seas Marine Life, Impact on Economic Sectors (VECTORS). The authors thank the various people and institutes that provided data: the GIP Seine-Aval and Marie Laure Cochard, Paul Marchal and Marie Savina-Rolland (Ifremer). We are grateful to Sophie Pasquier for compiling the references.

References

Anon. 1965. Report of the working group on sole. ICES Coop.Res. Rep. 5: 1-126.

Anon. 1989. Report of ad hoc study group on juvenile sole tagging. ICES CM 1989/G: 21, 34pp.

Archambault, B., Le Pape, O., Bousquet, N., and Rivot, E. 2014. Density-dependence can be revealed by modelling the variance in the stock–recruitment process: an application to flatfish. ICES J. Mar. Sci. 71(8): 2127–2140.

Botsford, L.W., Brumbaugh, D.R., Grimes, C., Kellner, J.B., Largier, J., O'Farrell, M.R., Ralston, S., Soulanille, E., and Wespestad, V. 2009. Connectivity, sustainability, and yield: bridging the gap between conventional fisheries management and marine protected areas. Rev. Fish Biol. Fish. 19: 69–95.

Buckland, S.T., Newman, K.B., Fernández, C., Thomas, L., and Harwood, J. 2007. Embedding population dynamics models in inference. Stat. Sci. 22(1): 44–58.

Burt, G. J., and Millner, R. S. 2008. Movements of sole in the southern North Sea and eastern English Channel from tagging studies (1955–2004). Sci. Ser. Tech. Rep. 44.

Brooks, S. P., and Gelman, A. 1998. General methods for monitoring convergence of iterative simulations. J. Comp. Graph. Stat. 7(4): 434–455.

Carruthers, T.R., McAllister, M.K., and Taylor, N.G. 2011. Spatial surplus production modeling of Atlantic tunas and billfish. Ecol. Appl. 21: 2734–2755.

Carson, H.S., Cook, G.S., López-Duarte, P.C., and Levin, L.A. 2011. Evaluating the importance of demographic connectivity in a marine metapopulation. Ecology 92: 1972–1984.

Chambers, R.C., and Trippel, E.A. 1997. Early life history and recruitment in fish populations. Chapman and Hall, New York.

Cianelli, L., Fisher, J., Skern-Mauritzen, M., Hunsicker, M., Hidalgo, M., Frank, K., and Bailey, K. 2013. Theory, consequences and evidence of eroding population spatial structure in harvested marine fishes: a review. Mar. Ecol. Prog. Ser. 480: 227–243.

Clark, J.S. 2005. Why environmental scientists are becoming Bayesians? Ecol. Lett. 8: 2–14.

Coggan, R.A., and Dando, P.R. 1988. Movements of juvenile Dover sole, Solea solea (L.), in the Tamar Estuary, South-western England. J. Fish Biol. 33: 177–184.

Conn, P.B., Williams, E.H., and Shertzer, K.W. 2010. When can we reliably estimate the productivity of fish stocks? Can. J. Fish. Aquat. Sci. 67:511–523.

Cowen, R.K., Lwiza, K.M.M., Sponaugle, S., Paris, C.B., and Olson, D.B. 2000. Connectivity of Marine Populations: Open or Closed? Science 287: 857–859.

Cunningham, C., Reid, D., McAllister, M., Kirkwood, G., and Darby, C. 2007. A Bayesian state-space model for mixed-stock migrations, with application to Northeast Atlantic mackerel Scomber scombrus. Afr. J. Mar. Sci. 29(3): 347-367.

Cuveliers, E.L., Geffen, A.J., Guelinckx, J., Raeymaekers, J.A.M., Skadal, J., Volckaert, F.A.M., and Maes, G.E. 2010. Microchemical variation in juvenile Solea solea otoliths as a powerful tool for studying connectivity in the North Sea. Mar. Ecol. Prog. Ser. 401: 211–220.

Cuveliers, E., Larmuseau, M., Hellemans, B., Verherstraeten, S., Volckaert, F., and Maes, G. 2012. Multi-marker estimate of genetic connectivity of sole (Solea solea) in the North-East Atlantic Ocean. Mar. Biol. 159: 1239–1253.

Darnaude, A., and Hunter, E. 2008. Coupled use of data storage tags and otolith microchemistry to assess population dispersal and intra-specific diversity in migratory behaviour in North Sea plaice (Pleuronectes platessa L.). Comp. Biochem. Phys. A 150: S205.

Diopere, E., Hellemans, B., Volckaert, F.A.M., and Maes, G.E. 2013. Identification and validation of single nucleotide polymorphisms in growth- and maturation-related candidate genes in sole (Solea solea L.). Mar. Genom. 9: 33–38.

Drouineau, H., Mahévas, S., Bertignac, M., and Duplisea, D. 2010. A length-structured spatially explicit model for estimating hake growth and migration rates. ICES J. Mar. Sci. 67(8) 1697–1709.

Exadactylos., A., Geffen, A.J., Panagiotaki, P., and Thorpe, J.P. 2003. Population structure of Dover sole Solea solea: RAPD and allozyme data indicate divergence in European stocks. Mar. Ecol. Prog. Ser. 246: 253–264.

Fairchild, E.A., Rennels, N., and Howell, H. 2009. Using telemetry to monitor movements and habitat use of cultured and wild juvenile winter flounder in a shallow estuary. In Tagging and Tracking of Marine Animals with Electronic Devices, Springer Netherlands. pp. 5–22.

Fodrie, F., and Herzka, S. 2013. A comparison of otolith geochemistry and stable isotope markers to track fish movement: describing estuarine ingress by larval and post-larval halibut. Estuar. Coast. 39: 906–917.

Frisk, M.G., Jordaan, A., and Miller, T.J. 2014. Moving beyond the current paradigm in marine population connectivity: are adults the missing link? Fish Fish. 15(2): 242-254.

Furey, N., Dance, M., and Rooker, J. 2013. Fine-scale movements and habitat use of juvenile southern flounder Paralichthys lethostigma in an estuarine seascape. J. Fish Biol. 82: 1469–1483.

Gaines, S.D., White, C., Carr, M.H., and Palumbi, S.R. 2010. Designing marine reserve networks for both conservation and fisheries management. P. Natl. Acad. Sci. 107: 18286–18293.

Gallego, A., North, E.W., and Houde, E.D. 2012. Understanding and quantifying mortality in pelagic, early life stages of marine organisms - Old challenges and new perspectives. J. Marine Syst. 93: 1–3.

Gelman, A. 2009. Bayes, Jeffreys, prior distributions and the philosophy of statistics. Stat. Sci. 24(2):176–178.

Gelman, A., Carlin, J.B., Stern, H.S., and Rubin, D.B. 2004. Bayesian Data Analysis. Chapman & Hall/CRC. 717 pp.

Gibson, R.N. 2004. Flatfishes: Biology and Exploitation. Wiley. 419 pp.

Goethel, D.R., Legault, C.M., and Cadrin, S.X. 2014. Demonstration of a spatially explicit, tag-integrated stock assessment model with application to three interconnected stocks of yellowtail flounder off of New England. ICES J. Mar. Sci. 72(1): 164–177.

Grosberg, R.K., and Levitan, D.R. 1992. For adults only? Supply-side ecology and the history of larval biology. Trends Ecol. Evol. 7: 130–133.

Grüss, A., Kaplan, D., Guenette, S., Roberts, C., and Botsford, L. 2011. Consequences of adults and juvenile movement for marine protected areas. Biol. Conserv. 144: 692–702.

Guan, W., Cao, J., Chen, Y., and Cieri, M. 2013. Impacts of population and fishery spatial structures on fishery stock assessment. Can. J. Fish. Aquat. Sci. 70: 1178–1189.

Hellberg, M.E., Burton, R.S., Neigel, J.E., and Palumbi, S.R. 2002. Genetic assessment of connectivity among marine populations. B. Mar. Sci. 70: 273–290.

Hilborn, R. 1990. Determination of Fish Movement Patterns from Tag Recoveries using Maximum Likelihood Estimators. Can. J. Fish. Aquat. Sci. 47: 635–643.

Hilborn, R., and Walters, C.J. 1992. Quantitative fisheries stock assessment: choice, dynamics and uncertainty. Rev. Fish Biol. Fisher. 2: 177–178.

Hinrichsen, H.-H., Dickey-Collas, M., Huret, M., Peck, M.A., and Vikebø, F.B. 2011. Evaluating the suitability of coupled biophysical models for fishery management. ICES J. Mar. Sci. 68: 1478–1487.

Hintzen, N.T., Roel, B., Benden, D., Clarke, M., Egan, A., Nash, R.D.M., Rohlf, N. and Hatfield, E. M. C. 2015. Managing a complex population structure: exploring the importance of information from fisheries-independent sources. ICES J. Mar. Sci. 72(2) : 528–542.

Hulson, P.J. F., Quinn, T.J., Hanselman, D.H. and Ianelli, J.N. 2013. Spatial modeling of Bering Sea walleye pollock with integrated age-structured assessment models in a changing environment. Can. J. Fish. Aquat. Sci. 70(9), 1402–1416.

ICES 2010. Report of the Working Group on the Assessment of Demersal Stocks in the North Sea and Skagerrak (WGNSSK), 5–11 May 2010. ICES CM 2010/ACOM:13. Copenhagen, ICES Headquarters, 1058 pp.

ICES. 2013. Report of the Working Group on the Assessment of Demersal Stocks in the North Sea and Skagerrak (WGNSSK), 24–30 April 2013, ICES Headquarters, Copenhagen. ICES Document CM 2013/ACOM:13. 1435 pp.

Iles, T.C., and Beverton, R.J.H. 2000. The concentration hypothesis: the statistical evidence. ICES J. Mar. Sci. 57: 216–227.

Korman, J., Martell, S.J.D., Walters, C.J., Makinster, A.S., Coggins, L.G., Yard, M.D., and Persons, W.R. 2012. Estimating recruitment dynamics and movement of rainbow trout (Oncorhynchus mykiss) in the Colorado River in Grand Canyon using an integrated assessment model. Can. J. Fish. Aquat. Sci. 69(11): 1827–1849.

Kotthaus, A. 1963. Tagging experiments with the North Sea sole (Solea solea) in 1959 and 1960. In Special Publication number 4 of the International Commission for the Northwest Atlantic Fisheries, pp. 123–129. Headquarters of the Commission, Darthmouth, Nova Scotia, Canada.

Le Pape, O., Chauvet, F., Mahévas, S., Lazure, P., Guérault, D., and Désaunay, Y. 2003a. Quantitative description of habitat suitability for the juvenile common sole (Solea solea, L.) in the Bay of Biscay (France) and the contribution of different habitats to the adult population. J. Sea Res. 50: 139–149.

Le Pape, O., Chauvet, F., Désaunay, Y., Guérault, G. 2003b. Relationship between interannual variations of the river plume and the extent of nursery grounds for the common sole (Solea solea, L.) in Vilaine Bay. Effects on recruitment variability. J. Sea Res. 50: 177-185.

Le Pape, O., and Bonhommeau, S. 2015. The food limitation hypothesis for juvenile marine fish. Fish Fish. 16(3): 373–398.

Le Pape, O. and Cognez, N. 2016. The range of juvenile movements of estuarine and coastal nursery dependent flatfishes: estimation from a meta-analytical approach. J. Sea Res. 107(1): 43-55

Levin, P.S., and Stunz, G.W. 2005. Habitat triage for exploited fishes: Can we identify essential 'Essential Fish Habitat?' Estuar. Coast. Shelf S. 64: 70–78.

Liebhold, A., Koenig, W. D., and Bjørnstad, O.N. 2004. Spatial synchrony in population dynamics. Annu. Rev. Ecol. Evol. S. 35(1) 467–490.

Massiot-Granier, F., Prévost, E., Chaput, G., Potter, T., Smith, G., White, J., Mantyniemi, S., Rivot, E. 2014. Embedding stock assessment within an integrated hierarchical Bayesian life cycle modelling framework: an application to Atlantic salmon in the Northeast Atlantic. ICES J. Mar. Sci. 71(7): 1653–1670.

McAllister, M., Hill, S., Agnew, D., Kirkwood, G., and Beddington, J. 2004. A Bayesian hierarchical formulation of the De Lury stock assessment model for abundance estimation of Falkland Islands' squid (Loligo gahi). Can. J. Fish. Aquat. Sci. 61:1048–1059.

Miller, T.J. 2007. Contribution of individual-based coupled physical-biological models to understanding recruitment in marine fish populations. Mar. Ecol. Prog. Ser. 347: 127–138.

Parent, E., and Rivot, E. 2013. Introduction to Hierarchical Bayesian Modeling for Ecological Data. Applied Environmental Statistics. Chapman & Hall/CRC. 427 pp.

Peck, M., and Hufnagl, M. 2012. Can IBMs tell us why most larvae die in the sea? Model sensitivities and scenarios reveal research needs. J. Marine Syst. 93: 77–93.

Petitgas, P., Rijnsdorp, A., Dickey-Collas, M., Engelhard, G., Peck, M., Pinnegar, J., Drinkwater, K., Huret, M., and Nash, R.D.M. 2013. Impacts of climate change on the complex life cycles of fish. Fish Oceanogr. 22: 121–139.

Planque, B., Loots, C., Petitgas, P., Lindstrom, U., and Vaz, S. 2011. Understanding what controls the spatial distribution of fish populations using a multi-model approach. Fish. Oceanogr. 20: 1–17.

Polacheck, T., Paige Eveson, J., and Laslett, G.M. 2010. Classifying tagging experiments for commercial fisheries into three fundamental types based on design, data requirements and estimable population parameters. Fish and Fish. 11(2): 133–148.

Punt, A.E., Hilborn, R. 1997. Fisheries stock assessment and decision analysis: the Bayesian approach. Rev. Fish Biol. Fisher. 7: 35–63.

Ranta, E., Kaitala, V., Lindström, J., and Helle, E. 1997. The Moran effect and synchrony in population dynamics. Oikos, 78(1): 136–142.

Rijnsdorp, A.D., and Pastoors, M.A. 1995. Modelling the spatial dynamics and fisheries of North Sea plaice (Pleuronectes platessa L.) based on tagging data. ICES J. Mar. Sci. 52: 963–980.

Rijnsdorp, A.D., Van Beek, F.A., Flatman, S., Millner, R.M., Riley, J.D., Giret, M., and De Clerck, R. 1992. Recruitment of sole stocks, Solea solea (L.), in the Northeast Atlantic. Neth. J. Sea Res. 29: 173–192.

Riou, P., Le Pape, O., and Rogers, S.I. 2001. Relative contributions of different sole and plaice nurseries to the adult population in the Eastern Channel : application of a combined method using generalized linear models and a geographic information system. Aquat. Living Resour. 14: 125–135.

Rivot, E., Prévost, E., Parent, E., and Baglinière, J.L. 2004. A Bayesian state-space modelling framework for fitting a salmon stage-structured population dynamic model to multiple time series of field data. Ecol. Model. 179: 463–485.

Rivot, E., Prévost, E. 2002. Hierarchical bayesian analysis of capture-mark-recapture data. Can. J. Fish. Aquat. Sci. 59: 1768–1784

Rochette, S., Huret, M., Rivot, E., and Le Pape, O. 2012. Coupling hydrodynamic and individual-based models to simulate long-term larval supply to coastal nursery areas. Fish. Oceanogr. 21: 229–242.

Rochette, S., Le Pape, O., Vigneau, J., and Rivot, E. 2013. A hierarchical Bayesian model for embedding larval drift and habitat models in integrated life cycles for exploited fish. Ecol. Appl. 23: 1659–1676.

Rochette, S., Rivot, E., Morin, J., Mackinson, S., Riou, P., and Le Pape, O. 2010. Effect of nursery habitat degradation on flatfish population: Application to Solea solea in the Eastern Channel (Western Europe). J. Sea Res. 64: 34–44.

Rolland, J.-L., Bonhomme, F., Lagardere, F., Hassan, M., and Guinand, B. 2007. Population structure of the common sole (Solea solea) in the Northeastern Atlantic and the Mediterranean Sea: revisiting the divide with EPIC markers. Mar. Biol. 151: 327–341.

Rooper, C.N., Gunderson, D.R., and Armstrong, D.A. 2004. Application of the concentration hypothesis to English sole in nursery estuaries and potential contribution to coastal fisheries. Estuaries 27: 102–111.

Ruiz, J., González-Quirós, R., Prieto, L., and Navarro, G. 2009. A Bayesian model for anchovy (Engraulis encrasicolus): the combined forcing of man and environment. Fish. Oceanogr. 18: 62–76.

Sackett, D.K., Able, K.W., and Grothues, T.M. 2008. Habitat dynamics of summer flounder Paralichthys dentatus within a shallow USA estuary, based on multiple approaches using acoustic telemetry. Mar. Ecol. Prog. Ser. 364: 199–212.

Savina, M., Lacroix, G., and Ruddick, K. 2010. Modelling the transport of common sole larvae in the southern North Sea: Influence of hydrodynamics and larval vertical movements. J. Marine Syst. 81: 86–98.

Savina, M., Lunghi, M., Archambault, B., Baulier, L., Huret, M., and Le Pape, O. *in press*. Sole larval supply to coastal nurseries: Interannual variability and connectivity at interregional and interpopulation scales. J. Sea. Res. http://doi.org/10.1016/j.seares.2015.11.010.

Selkoe, K., Henzler, C., and Gaines, S. 2008. Seascape genetics and the spatial ecology of marine populations. Fish and Fish. 9: 363–377.

Smedbol, R.K., McPherson, A., Hansen, M.M., and Kenchington, E. 2002. Myths and moderation in marine 'metapopulations'? Fish Fish. 3: 20–35.

Spiegelhalter, D.J., Best, N.G., Carlin, B.P., and van der Linde, A. 2014. The deviance information criterion: 12 years on. J. Roy. Statist. Soc. Ser. B. 76(3): 485–493.

Stelzenmuller, V., Schulze, T.F.H.O., and Berkenhagen, J. 2011. Integrating modelling tools to support risk-based decision-making in marine spatial management. Mar. Ecol. Prog. Ser. 441: 197–212.

Strathmann, R.R., Hughes, T.P., Kuris, A.M., Lindeman, K.C., Morgan, S.G., Pandolfi, J.M., and Warner, R.R. 2002. Evolution of local recruitment and its consequences for marine populations. B. Mar. Sci. 70: 377–396.

Taylor, N.G., McAllister, M.K., Lawson, G.L., Carruthers, T., and Block, B.A. 2011. Atlantic bluefin tuna: A novel multistock spatial model for assessing population biomass. PLoS One 6(12): e27693.

Tidd, A.N., Vermard, Y., Marchal, P., Pinnegar, J, Blanchard, J.L., Milner-Gulland E.J. 2015. Fishing for space: Fine-scale multi-sector maritime activities influence fisher location choice. PLos One 10(1): e0116335.

Tuck, G., and Possingham, H. 1994. Optimal harvesting strategies for a metapopulation. B. Math. Biol. 56(1): 107–127.

Vasconcelos, R., Eggleston, D.B., Le Pape, O., Tulp, I. 2014. Patterns and processes of habitat-specific demographic variability in exploited marine species. ICES J. Mar. Sci. 71: 638-647.

Waples, R.S. 1998. Separating the wheat from the chaff: patterns of genetic differentiation in high gene flow species. J. Hered. 89: 438–450.

Ward, R.D., Woodwark, M., and Skibinski, D.O.F. 1994. A comparison of genetic diversity levels in marine, freshwater, and anadromous fishes. J. Fish Biol. 44: 213–232.

Warner, R.R., and Cowen, R.K. 2002. Local retention of production in marine populations: Evidence, mechanisms, and consequences. B. Mar. Sci. 70: 245–249.

Wolfshaar, K. E. van de, HilleRisLambers, R., and Grdmark, A. 2011. Effect of habitat productivity and exploitation on populations with complex life cycles. Mar. Ecol. Prog. Ser. 438: 175–184.

Yau, A.J., Lenihan, H.S., and Kendall, B.E. 2014. Fishery management priorities vary with self-recruitment in sedentary marine populations. Ecol. Appl. 24(6): 1490–1504.

Ying, Y., Chen, Y., Lin, L., Gao, T., and Quinn, T. 2011. Risks of ignoring fish population spatial structure in fisheries management. Can. J. Fish. Aquat. Sci. 68: 2101–2120.

Appendix A

Equations for the Hierarchical Bayesian Life-cycle Model

The equation below stand for the model considering three loosely connected subpopulations. The model is written in a state-space form that integrates stochasticity in both the process equations of the population dynamics (process errors) and the observation equations (observation errors). Following this logic, the appendix below first provides the equation for the population dynamics and then provides the equation for the observation process.

Subscript y denotes the years in the time series, i denotes the nursery sector (i=1,…,5, with 1=Seine, 2=Veys, 3= UK West, 4=Rye, 5=Somme), and r denotes the component of the metapopulation (r=1,2,3 with 1=West FR, associated with nursery grounds Seine and Veys; 2=UK, associated with nursery grounds UK West and Rye; 3=East FR, associated with nursery ground Somme).

Prior distribution or fixed values for parameters are defined in Table A1. The surface of each nursery sector (in km^2) is given in Table A.2.

Process equations

Eggs and larval drift

The number of settling larvae (i.e., post-larvae) in nursery sector i at year y, $L_{y,i}$, is defined as follows:

(A.1) $$L_{y,i} = \sum_{r=1}^{r=3} \omega_{y,r} \cdot D_{y,r,i}$$

where $\omega_{y,r}$ is the egg pool for the subpopulation r at year y and $D_{y,r,i}$ is the probability of success for an egg from the egg pool r to reach the nursery sector i at year y (fixed). The egg pool for each year and each subpopulation is calculated from the spawning stock biomass (all fish between age 3 and 15 take part in reproduction; ICES (2010)):

(A.2) $$\omega_{y,r} = \sum_{a \geq 3} N_{a,y,r} \cdot pf_a \cdot fec_{a,y}$$

where pf_a is the proportion of females for age class a (known, considered constant over the time series and homogeneous across areas), and $fec_{a,y}$ is the number of eggs per female of age a, calculated from the weight at age $w_{a,y}$ as (ICES, 2010; Rochette et al., 2012):

(A.3) $$fec_{a,y} = e^{5.6 + 1.17 * \log(w_{a,y})}$$

Post-larvae to juvenile on nursery grounds, from settlement to summer's end

The expected number of age-0 fish at year y in nursery i, $E(N_{0_{y,i}})$, is defined from a density dependent lognormally distributed around an expected mean defined from a Beverton-Holt equation parameterized with α_i, the nursery-specific maximum survival rate (estimated); K_i , the nursery-specific carrying capacity per unit of surface (1000 fish$\cdot$ km^{-2}, estimated); and S_i, the surface of nursery sector i (km^2, fixed; Tab. A.2):

$$\text{(A.4)} \qquad E(N_{0_{y,i}}) = \frac{\alpha_i \cdot L_{y,i}}{1+\frac{\alpha_i}{K_i \cdot S_i} \cdot L_{y,i}}$$

Unexplained random variations are captured by independent lognormal random noise with the same variance σ_{BH}^2 for all nurseries (estimated):

$$\text{(A.5)} \qquad N_{0,y,i} = E(N_{0_{y,i}}) \cdot e^{\varepsilon_{L,y,i} - 0.5 \cdot \sigma_{BH}^2}$$

Natural mortality of age 0 from summer's end to December

The number of age-1 fish in nursery i, $N_{1,y+1,i}$, is defined as

$$\text{(A.6)} \qquad N_{1,y+1,i} = N_{0,y,i} \cdot e^{-1/3 \cdot M_0} \cdot e^{\varepsilon_{0,y,i} - 0.5 \cdot \sigma_0^2}$$

where $N_{0,y,i}$ is the number of age-0 fish in the nursery i, M_0 is the annual natural mortality rate at age 0 (fixed) and $\varepsilon_{0,y,i}$ is normal environmental noise with variance σ_0^2(estimated).

Natural and fishing mortality at age 1 and emigration from nursery to adult population

The number of age-2 fish in nursery i at the very beginning of year $y+1$, $N_{2,y+1,i}$, is defined as

$$\text{(A.7)} \qquad N_{2,y+1,i} = N_{1,y,i} . e^{-Z_{1,y,i}} \cdot e^{\varepsilon_{1,y,i} - 0.5 \cdot \sigma_p^2}$$

where $Z_{1,y,i} = M_1 + F_{1,y,r}$ is the total mortality, M_1 is the annual natural mortality rate at age 1 (fixed), $F_{1,y,r}$ is the fishing mortality in subpopulation r associated with nursery i (estimated), and $\varepsilon_{1,y,i}$ is normal environmental noise with variance σ_p^2.

Age-2 fish leave nurseries at the very beginning of the year and are supposed to contribute directly to the subpopulation r adjacent to the nursery. Fish from the Seine and Veys nurseries contribute to subpopulation r=1=West FR; UK West and Rye nurseries contribute to subpopulation r=2=UK; and the Somme nursery contributes to subpopulation r=3=East FR. Starting from $N_{2,y+1,i}$ as defined in eq. (A.7), the number of age-2 fish in each subpopulation r, $N_{2,y+1,r}$ (note the subscript r and not i), is defined as follows:

$$\text{(A.8)} \qquad \begin{cases} N_{2,y+1,r=1} = \sum_{i=1}^{i=2} N_{2,y+1,i} \\ N_{2,y+1,r=2} = \sum_{i=3}^{i=4} N_{2,y+1,i} \\ N_{2,y+1,r=3} = N_{2,y+1,i=5} \end{cases}$$

Natural and fishing mortality at the adult stage

The number of fish from age 2 to 15 then follows the classical dynamics:

$$\text{(A.9)} \qquad N_{a+1,y+1,r} = N_{a,y,r} . e^{-Z_{a,y,r}} \cdot e^{\varepsilon_{a,y,r} - 0.5 \cdot \sigma_p^2}$$

where $N_{a,y,r}$ is the number of fish of age a in component r at year y, $Z_{a,y,r}$ is the total mortality rate and $\varepsilon_{a,y,r}$ is a normal environmental noise with variance σ_p^2. All remaining fish are assumed to die at age 15.

Model for total mortality Z

$Z_{a,y,r}$ is defined as the sum of natural mortality M_a, considered constant across years and subpopulations (Tab. A.1), and fishing mortality $F_{a,y,r}$. For any given age, year and subpopulation r, the expected mean of the fishing mortality is defined as $E(F_{a,y,r}) = S_a \cdot E_{y,r}$ with S_a as an age-specific selectivity (logistic function considered homogeneous in time and space, estimated, Tab. A.1) and $E_{y,r}$ as the fishing effort specific to each year and subpopulation. The time variability of fishing effort $E_{y,r}$ was a priori modeled as a random walk in the log-scale (Tab. A.1). Additional random variability of $F_{a,y,r}$ around the expected mean $E(F_{a,y,r})$ was captured through a random gamma hierarchical structure with the coefficient of variation CV_F (Tab A.1).

Observation equations

Juvenile abundance indices

The abundance indices of age-0 and age-1 juveniles in nursery i are considered as lognormal random observations of abundance $N_{0,y,i}$ and $N_{1,y,i}$, respectively:

(A.10) $$I_{0,y,i} = q_0 \cdot N_{0,y,i} \cdot e^{\varepsilon_{I_0,y,i} - 0.5\cdot\sigma^2_{I_{juv}}}$$

(A.11) $$I_{1,y,i} = q_1 \cdot N_{1,y,i} \cdot e^{\varepsilon_{I_1,y,i} - 0.5\cdot\sigma^2_{I_{juv}}}$$

with q_0 and q_1 the age-specific catchability, $\varepsilon_{I_0,y,i}$ and $\varepsilon_{I_1,y,i}$ independent normal random noise with the same observation error variance $\sigma^2_{I_{juv}}$ (estimated).

Adult abundance indices

In the model considering three subpopulations, three time series of abundance indices (AI) of age-2 to age-15 fish are used: CPUEs from the UK and Belgium commercial fleet (UKBCT and BEBCT, respectively), both of which are available on the scale of the entire Eastern Channel, and UK bottom-trawl surveys available for each subpopulations ($r = 1,2,3$). One observation equation is written for each AI, with each observation equation contributing to the whole likelihood function. The same general form of observation equation is used for all AIs, which are all considered as lognormal random observations of the abundance at age but with parameters specific for the fleet (UKBCT, BEBCT, UKBTS) age, year (and eventually subpopulation for UKBTS):

(A.12) $$AI_{fleet_{a,y,(r)}} = q_{fleet} \cdot S_a \cdot N_{a_{y,i,(r)}} \cdot e^{\varepsilon_{\text{fleet},a,y,(r)} - 0.5\cdot\sigma^2_{I_{Ad}}}$$

where $AI_{fleet_{a,y,(r)}}$ is the observed AI of age a at year y on a different spatial scale (in subpopulations r for the UKBTS survey; in the whole EC for other indices),q_{fleet} is the fleet-specific catchability, S_a is the age-specific selectivity (considered homogeneous among fleets), and $\varepsilon_{\text{fleet},a,y,(r)}$ is independent random noise with the same observation error variance $\sigma^2_{I_{Ad}}$ (estimated; homogeneous among fleets).

Catches-at-age aggregated on the scale of the Eastern Channel

Catches-at-age predicted by the model ($H_{a,y,r}$) were calculated for each subpopulation with the standard Baranov equation:

(A.13) $$H_{a,y,r} = N_{a,y,r} \cdot \left(\frac{F_{a,y,r}}{F_{a,y,r}+M_a}\right) \cdot \left(1 - e^{-(F_{a,y,r}+M_a)}\right)$$

Annual catches-at-age ($C_{a,y}$; observed) were available from stock assessment reports only on the scale of the Eastern Channel; however, they were not available separately for the three subpopulations. Catches-at-age predicted by the model were then first aggregated at the scale of the Eastern Channel ($H_{a,y} = \sum_{r=1}^{r=3} H_{a,y,r}$) and considered observed with lognormal errors:

(A.14) $$C_{a,y} = H_{a,y} \cdot e^{\varepsilon_{Ca,y} - 0.5 \cdot \sigma_C^2}$$

where $\varepsilon_{Ca,y}$ are independent normal random noise with observation error variance σ_C^2 (estimated).

Spatial repartition of catches (weight) among subpopulations

A likelihood function for the catch weight ratio per subpopulation ($pw_{t,r}, \sum_{r=1:3} pw_{t,r} = 1$) was also incorporated into the model. The catch weight ratio was originally available using the ICES statistical rectangle from 2003 to 2011; however, it was here aggregated at the scale of the three areas associated with each subpopulation. Before 2003, the catch weight ratio per subpopulation was derived from the catch ratio per country (weight; known for the entire time series) combined with the average repartition of catches (weight) among the three areas calculated for each country over the most recent time series 2003-2011. This procedure only assumes a constant spatial repartition of national fleets among the three areas and is a reasonable hypothesis because no major change in the national fleet strategies has been observed between 1982 and 2011 (Y. Vermard, com. Pers.). The catch ratio predicted by the model ($\pi_{y,r}$) was calculated from the catches-at-age predicted by the model ($C_{a,y,r}$) and the weight-at-age ($w_{a,y}$; observed). A Dirichlet likelihood function was used to capture observation errors between the observed and predicted catch ratio. The predicted catch weight ratio was scaled to mimic the precision that would be obtained with a sample of 500 tones:

(A.15) $$\left(pw_{t,r=1}, pw_{t,r=2}, pw_{t,r=2}\right) \sim \text{Dirichlet}\left(500 \times \left(\pi_{t,r=1}, \pi_{t,r=2}, \pi_{t,r=3}\right)\right)$$

Parameters and priors

Prior distributions or fixed values of parameters are given in Tab. A1.

Following Rochette et al. (2013), informative priors were set for parameters of the selectivity S_a, based on ICES (2013). The priors on the carrying capacity of nursery sectors, K_i's, were weakly informative in the sense of Gelman (2009), i.e., it allows the data to speak while being strong enough to exclude unrealistic values (the 90% percentile of the prior predictive distribution is more than 100 times greater than the highest estimated density in nurseries of the Bay of Biscay; Le Pape et al., 2003a).

Informative priors were set on the nursery-specific maximum survival rates α_i. Taking away the EC sole dataset from the database used for the meta-analysis in Archambault et al. (2014), the posterior predictive distribution of α was derived and considered to build an informative prior for this study. The method developed in Archambault et al. (2014) provides a predictive distribution for the slope at origin calculated from a Beverton-Holt relationship calculated from egg-to-egg (denoted α_{meta}). By contrast, parameter α in our model (denoted α_{HBM}) stands for the survival rate from settled larvae to 0+ juveniles (in September). To transfer the information from α_{meta} to α_{HBM}, average demographic parameters specific to the Eastern Channel were used to complete the life cycle from the age-0 juveniles in September to eggs:

(A.16) $$S_{\omega-L} \cdot \alpha_{HBM} \cdot e^{-M_0 \cdot 4/12} \cdot \overline{Fec} \cdot SPR_{F=0} = \alpha_{meta}$$

with $S_{\omega-L}$ as the average eggs to post-larvae survival, $\overline{Fec}$ as the average fecundity, $SPR_{F=0}$ the spawning biomass produced in the absence of fishing and $e^{-M_0 \cdot 4/12}$ as the natural mortality from observation in September to recruitment at age 1 in January. Finally, because the meta-analysis of Archambault et al. (2014) was derived using recruitment estimated by ICES (recruitment at age 1 back-calculated from age 2), we also took into account the differences between the mortality used by ICES ($M_{1_{ICES}}$=0.1) and the one used in our model ($M_{1_{HBM}}$=2.6). The following final equation was then used to scale the posterior predictive of α_{meta} to obtain the informative prior of α_{HBM}:

(A.17) $$\alpha_{HBM} = \frac{\alpha_{meta}}{S_{\omega-L} \cdot e^{-M_0 \cdot 4/12} \cdot Fec \cdot SPR_{F=0}} \cdot e^{M_{1_{HBM}} - M_{1_{ICES}}}$$

Table A.1. Prior distribution (or fixed values) for the parameters of the Hierarchical Bayesian Life-cycle Model.

Parameters	**Value / prior / structure**	**Description**
M_a	Age 0: 1.5; Age 1: 2.6 ; Age 3-11: 0.1 ; Age 12: 0.2 ; Age 13: 0.3 ; Age 14: 0.4 ; Age 15: 0.5	Natural mortality at age a (y^{-1})
S_a	$a_{50} \sim Gamma(E = 3, CV = 0.1)$ $\delta \sim Gamma(E = 1, CV = 0.2)$	Age-specific gear selectivity. Logistic curve parameterized with (a_{50}, δ). a_{50} : the age at which $S_a = 0.5$; δ : the difference (in years) between $S_a = 0.25$ and $S_a = 0.75$. S_a is scaled to 1 for a=15.
σ_p^2	$\sigma_p^2 = 0.001$	Variance of process errors on the dynamics of adult stages (fixed to a very low value)
$E_{y,r}$	$log(E_{y=1,r}) \sim Norm(E = 0, \sigma = \sqrt{10})$ $\log(E_{y,r}) \sim Norm(E = log(E_{y-1,r}), \sigma_E))$ $\sigma_E \sim Unif(0.01,0.5)$	Fishing effort. Prior defined as a random walk in the log-scale
$F_{a,y,r}$	$F_{a,y,r} \sim Gamma(E = E_{y,r} \cdot S_a, CV_F)$ $CV_F \sim Unif(0,1)$	Fishing mortality Exchangeable hierarchical structure
α_i	$log(\alpha_i) \sim Norm(E = \mu_{log\alpha}, \sigma = \sigma_{log\alpha})[,0]$ $\mu_{log\alpha} \sim Norm(E = -3, \sigma = \sqrt{0.1})$ $\sigma_{log\alpha} \sim Unif(0,2.5)$	Nursery-specific maximum survival rates. Hierarchical structure with informative priors derived from Archambault et al. (2014)
K_i	$K_i \sim Norm(E = \mu_K, \sigma = \sigma_K)1_{>0}$ $\mu_K \sim Norm(E = 100, \sigma = 100)$ $\sigma_K \sim Unif(10,300)$	Nursery-specific carrying capacity per unit of surface (1000 fish·km^{-2}). Hierarchical structure with weakly informative priors
σ_{BH}^2	$log(\sigma^2{}_{BH}) \sim Unif(-10,10)$	Variance of process errors on the post-larvae to juvenile BH relationship
σ_0^2	$\log(\sigma^2{}_0) \sim Unif(-10,10)$	Variance of process errors from age-0 to age-1 fish
$\sigma_{I_{juv}}^2$	$\sigma_{I_{juv}}^2 \sim Unif(-10,10)$	Variance of observation errors on surveys of juveniles on nurseries
$\sigma_{I_{Ad}}^2$	$\sigma_{I_{Ad}}^2 \sim Unif(-10,10)$	Variance of observation errors on all abundance indices of adults (UKCBT, BECBT, UKBTS)
σ_C^2	$\sigma_C^2 \sim Unif(-10,10)$	Variance of observation errors on catches
q_0	$log(q_0) \sim Unif(-10,10)$	Catchability of age-0
q_1	$log(q_1) \sim Unif(-10,10)$	Catchability of age-1
q_{fleet}	$log(q_{fleet}) \sim Unif(-10,10)$	Catchability related to abundance indices of adults (fleet: UKCBT, BECBT, UKBTS)

Table A.2. Surface of nursery sector i (km^2). All surfaces are derived from the habitat suitability model in Rochette et al. (2010).

Subpopulation	**Nursery sector**	**Surface** (km^2)
West Fr ($r = 1$)	Seine ($i = 1$)	967
	Veys ($i = 2$)	320
UK ($r = 2$)	UK West ($i = 3$)	1,650
	Rye ($i = 4$)	504
East FR ($r = 3$)	Somme ($i = 5$)	1,680

Appendix B

Catches at equilibrium as a function of fishing mortality

Empirical equilibrium curves were obtained by Monte Carlo simulations. The population was simulated with constant F in time and space during 200 years to reach an equilibrium state. Results obtained by varying F in a wide range (from 0 to 2, with a step of 0.01) were used to empirically construct the equilibrium curve relating Catches and SSB at equilibrium, thus enabling the estimation of management reference points such as B_{MSY}, F_{MSY} and C_{MSY}. Drift and survival parameters for eggs and larvae were considered constant during the simulations and set to their average values (1982-2007). In the model considering three subpopulations, reference equilibrium points for each subpopulation r (denoted $B_{MSY,r}$, $F_{MSY,r}$ and $C_{MSY,r}$) were estimated conditionally by fixing the fishing pressure for the two other subpopulations equal to the estimates averaged over the last five years of the data series (2007-2011).

Monte Carlo simulations were run to account for both process errors and parameters uncertainty. For a given value of F, the population dynamics was simulated over 200 years, including process error. The equilibrium (ergodic) state is considered after 100 years of simulation and the process error was integrated out by considering the distribution of the results between year 101 and 200. To integrate the parameter uncertainty, the procedure was repeated 1,500 times with 1,500 sets of parameters directly drawn in the joint posterior distribution of model parameters, ensuring that the statistical covariance structure between the parameters is fully accounted for (Punt and Hilborn, 1997; Parent and Rivot, 2013).

Supplementary Material S1

MCMC simulations and convergence diagnosis

Bayesian posterior distributions were approximated via Monte Carlo Markov Chain (MCMC) methods using the JAGS software (http://mcmc-jags.sourceforge.net ; release 3.4.0) through the Rjags (www.Rproject.org) package. The same procedure detailed below was used for all model configurations.

Following the seminal idea of Meyer and Millar (1999) who proposed a parameterization of the biomass dynamic production model in terms of biomass relative to the carrying capacity to improve the convergence speed of the MCMC sampler, equations for the cohort dynamics (eqs. A.7 and A.9) in the JAGS code was written with numbers at age relative to the recruitment of the cohort measured at age 1.

Three MCMC-independent chains with dispersed initialization points were used. For each chain, the first 10,000 iterations were first discarded. The three chains were run during 10^6 iterations. Autocorrelation in the MCMC sampling process was rather high (> 0.5 at lag 50 for almost all variables). To reduce the autocorrelation in the sample used for inferences, one out of 100 iterations was kept (thinning = 100). The autocorrelation in the resulting thinned chained was less than 0.2 for all variables. Final inferences were derived from a sample of $3\times10{,}000$ iterations resulting from merging the three chains.

Convergence of the MCMC chains was assessed using the Gelman-Rubin (Brooks and Gelman, 1998) and the Heidelberg and Welch tests as implemented in the R Coda package (gelman.diag() and heidel.diag() function, respectively). The Gelman-Rubin tests for the mixing of multiple chains. It is based on the computation of the R-ratio that compares within and between-chain variances. Values of the R-ratio substantially above 1 indicate lack of convergence. The Heidelberg and Welch diagnostic is a “single chain diagnostic” that calculates a statistics to test for the null hypothesis that the chain is from a stationary distribution.

For both models, trace plot display good mixing for all variables (see examples in Fig. S1.1). All variables pass the two convergence diagnostics. The R ratio of the Gelman Rubin test was < 1.05 for all variables and p-values of the Heidelberg test were all < 0.05. However, it is worth noting that convergence was more difficult to achieve for the parameters of the BevHolt density dependence recruitment process associated with nursery sector “Bay of Veys” for which the juveniles abundance indices are only available for 3 years.

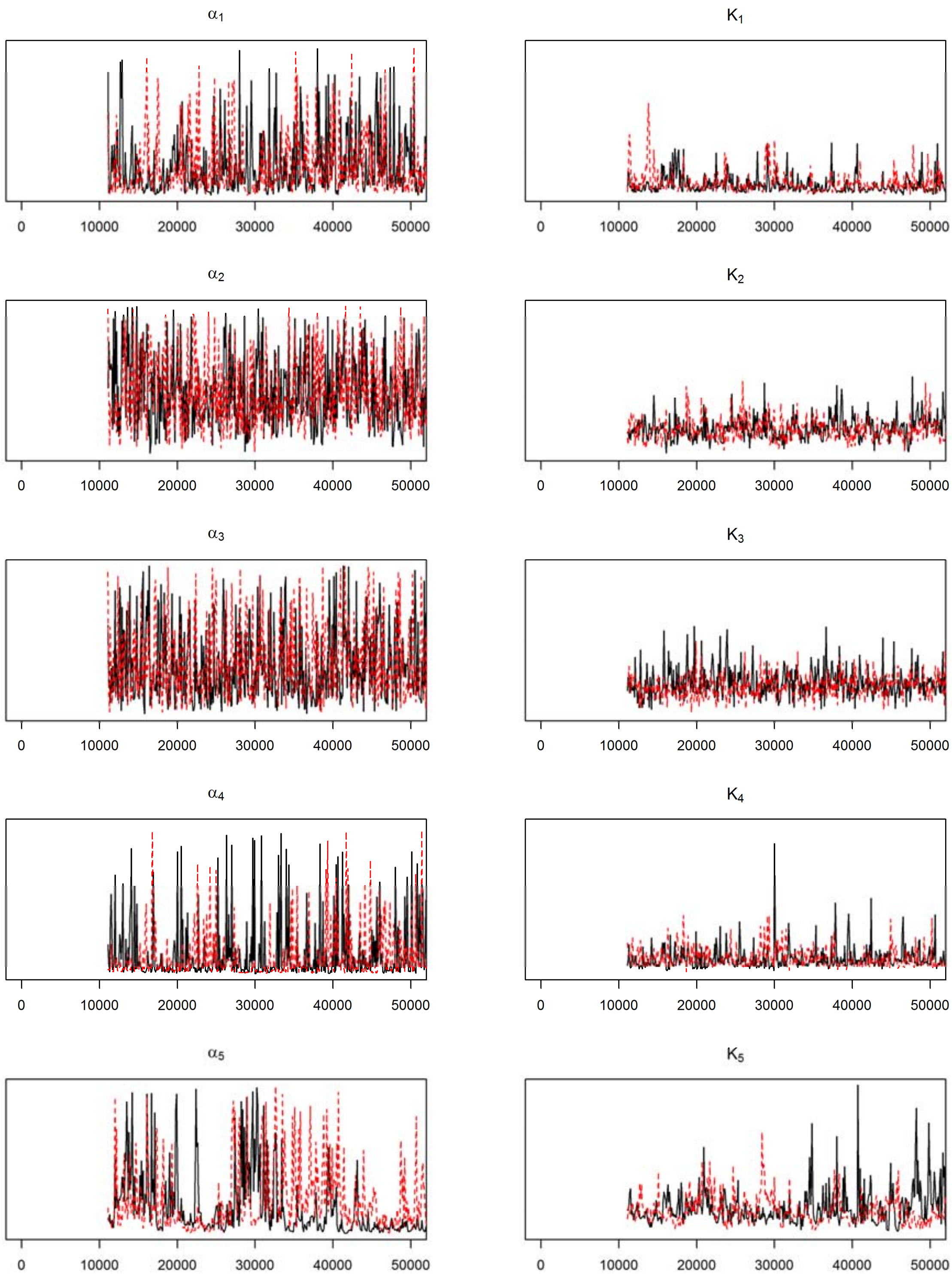

Fig. S1.1. Trace plots of Beverton-Holt parameters (α_i, K_i) in the 5 nursery sectors (for the model considering three sub-populations). To keep the figure as clear as possible, trace plots are drawn for two independent chains (out of three) and for the first 100 000 iterations (out of a total of 10^6). But final inferences have been drawn from longer MCMC chains of length 10^6.

Supplementary Material S2

Posterior predictive distribution for the different sources of observations in the model considering three subpopulations.

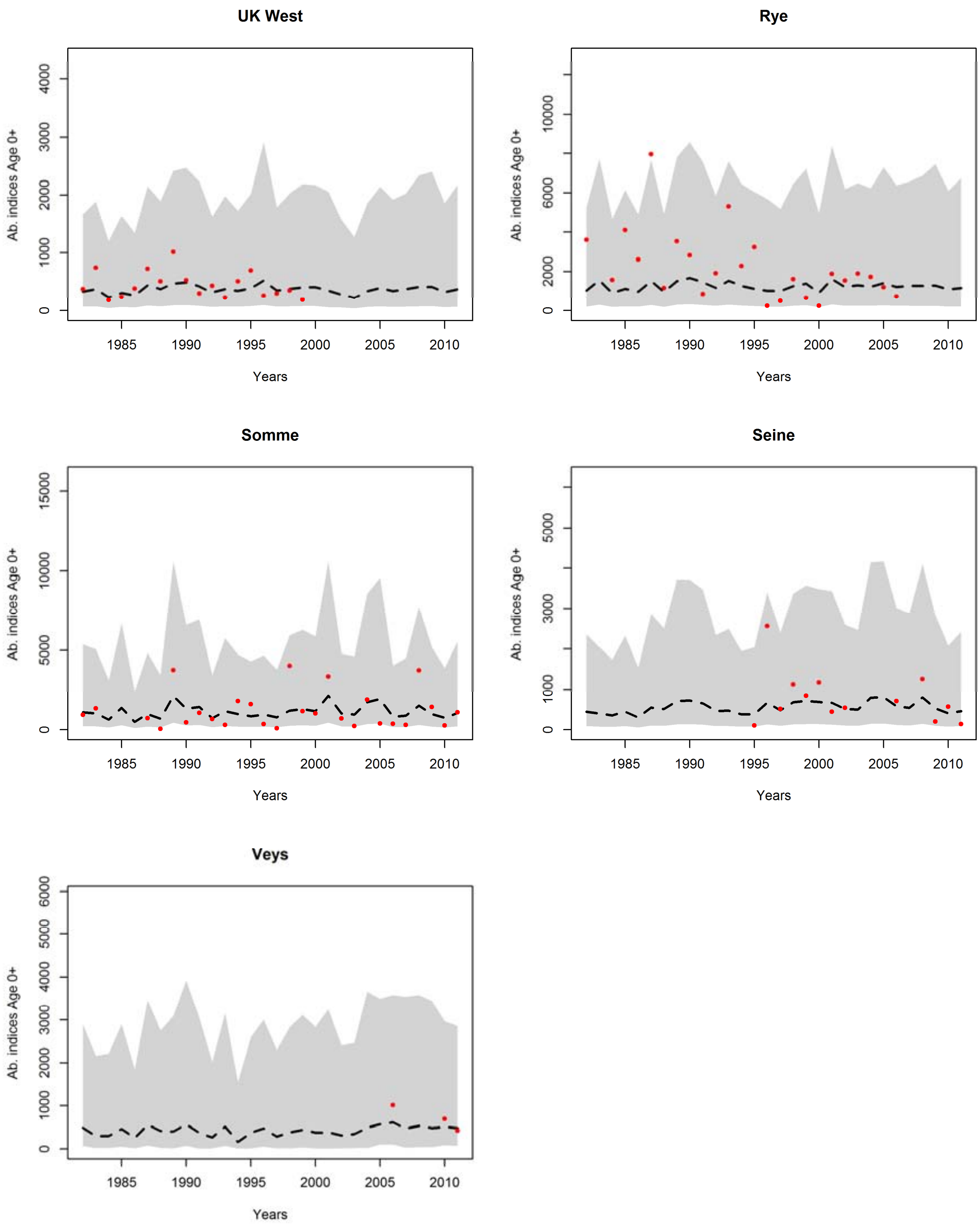

Fig. S2.1. Posterior predictive distribution and observations for Age-0 abundance indices in the five nursery sectors. Dots : Observations; Dotted lines: medians of the posterior predictive distribution; Shaded areas: 90% Bayesian credible intervals for the posterior predictive distribution.

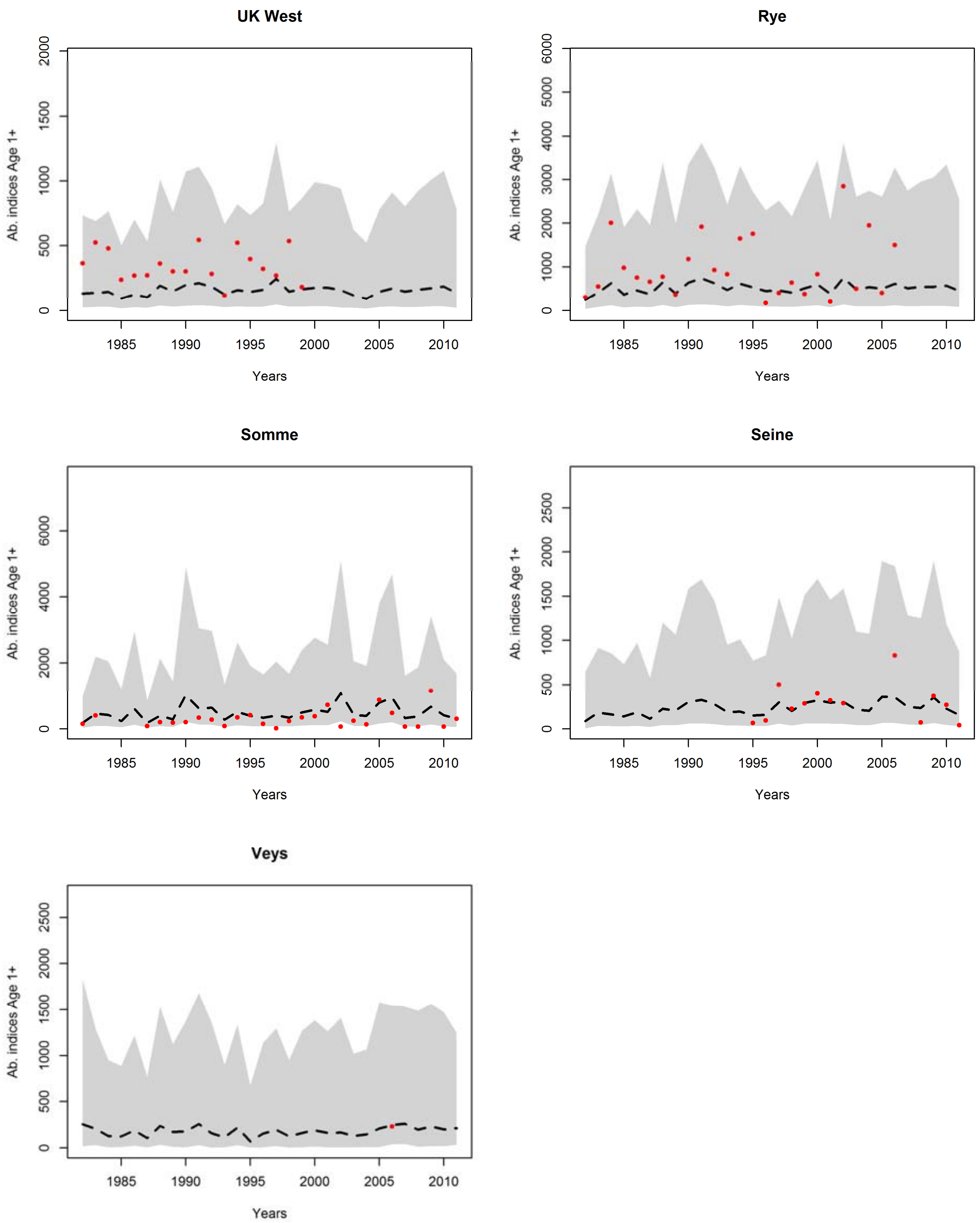

Fig. S2.2. Posterior predictive distribution and observations for Age-1 abundance indices in the five nursery sectors. Dots : Observations; Dotted lines: medians of the posterior predictive distribution; Shaded areas: 90% Bayesian credible intervals for the posterior predictive distribution.

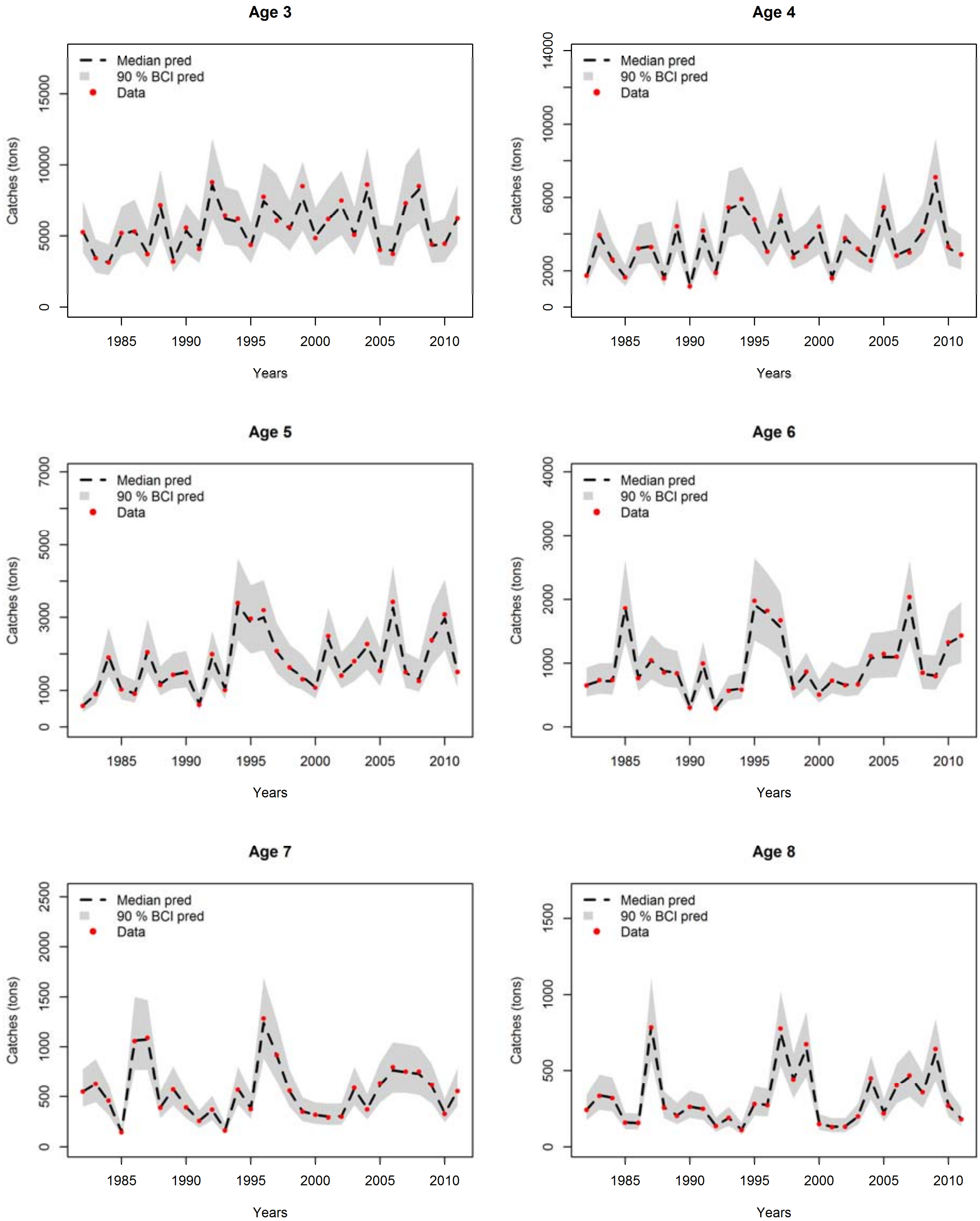

Fig. S2.3. Posterior predictive distribution and observations for catches (tons) of age-3 to age-8 fish in the Eastern Channel. Dots : Observations; Dotted lines: medians of the posterior predictive distribution; Shaded areas: 90% Bayesian credible intervals for the posterior predictive distribution.

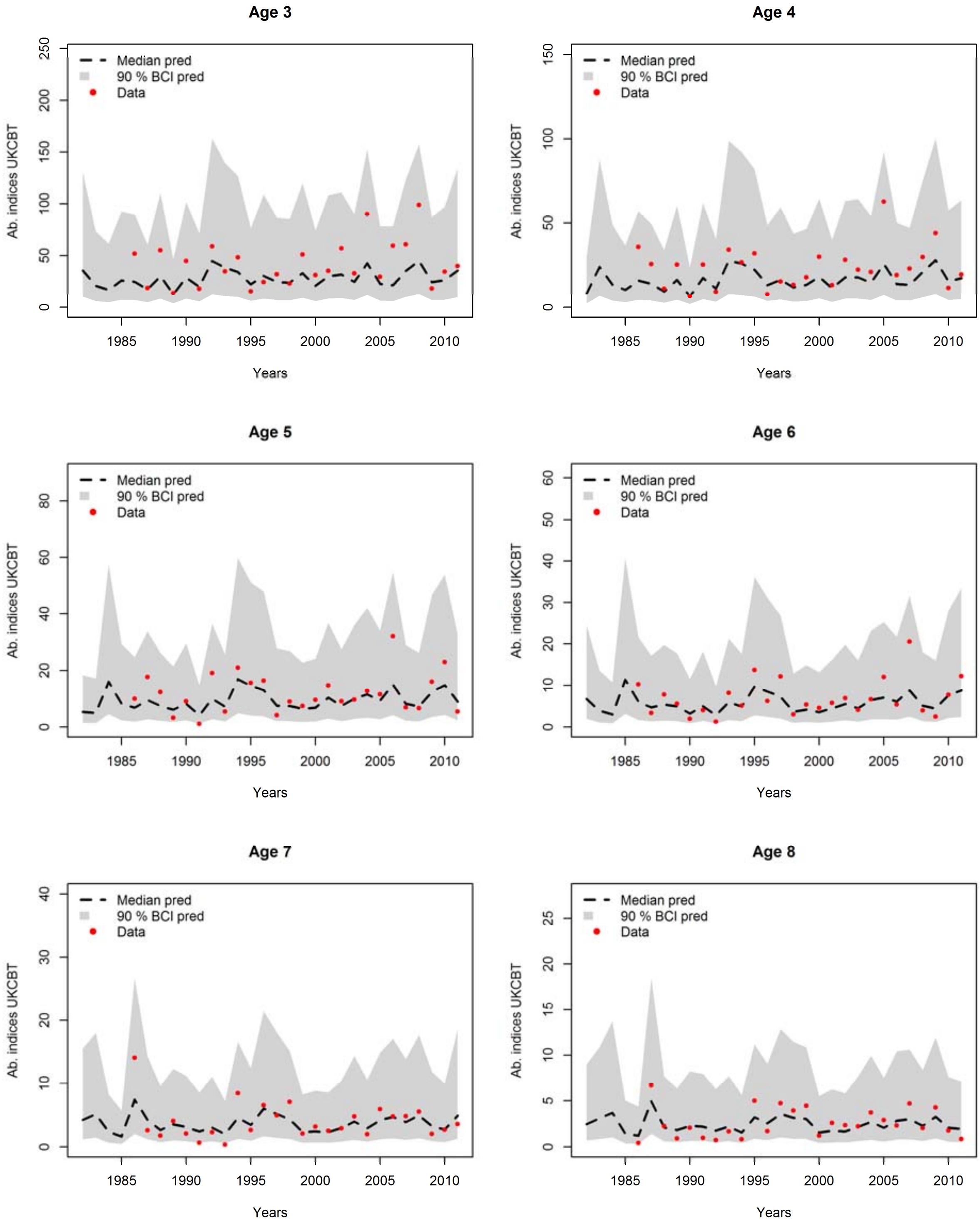

Fig. S2.4. Posterior predictive distribution and observations for commercial abundance indices UKCBT (age-3 to age-8 fish) in the Eastern Channel. Dots : Observations; Dotted lines: medians of the posterior predictive distribution; Shaded areas: 90% Bayesian credible intervals for the posterior predictive distribution.

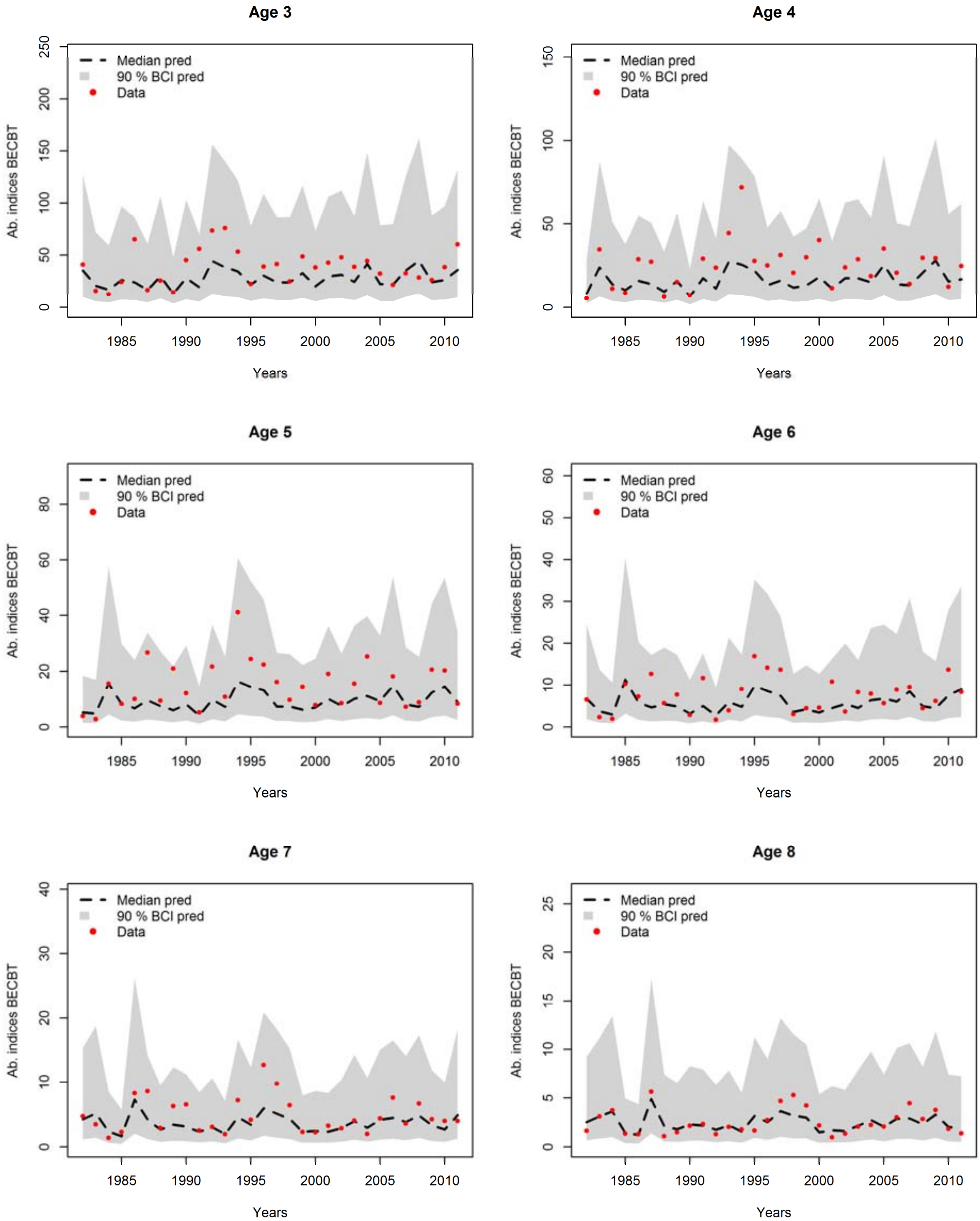

Fig. S2.5. Posterior predictive distribution and observations for commercial abundance indices BECBT (age-3 to age-8 fish) in the Eastern Channel. Dots : Observations; Dotted lines: medians of the posterior predictive distribution; Shaded areas: 90% Bayesian credible intervals for the posterior predictive distribution.

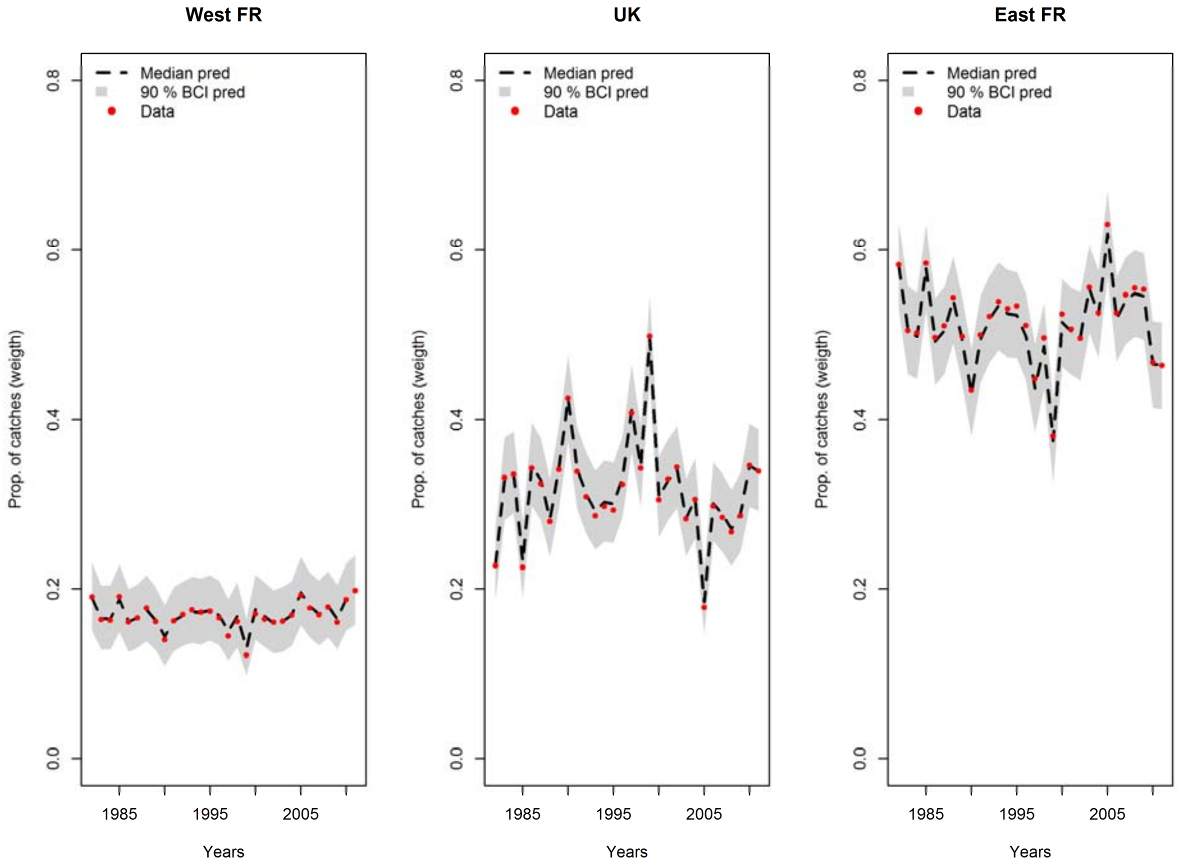

Fig. S2.6. Posterior predictive distribution and observations for the proportion of catches (total weight) in the three areas considered in the Eastern Channel. Dots : Observations; Dotted lines: medians of the posterior predictive distribution; Shaded areas: 90% Bayesian credible intervals for the posterior predictive distribution.

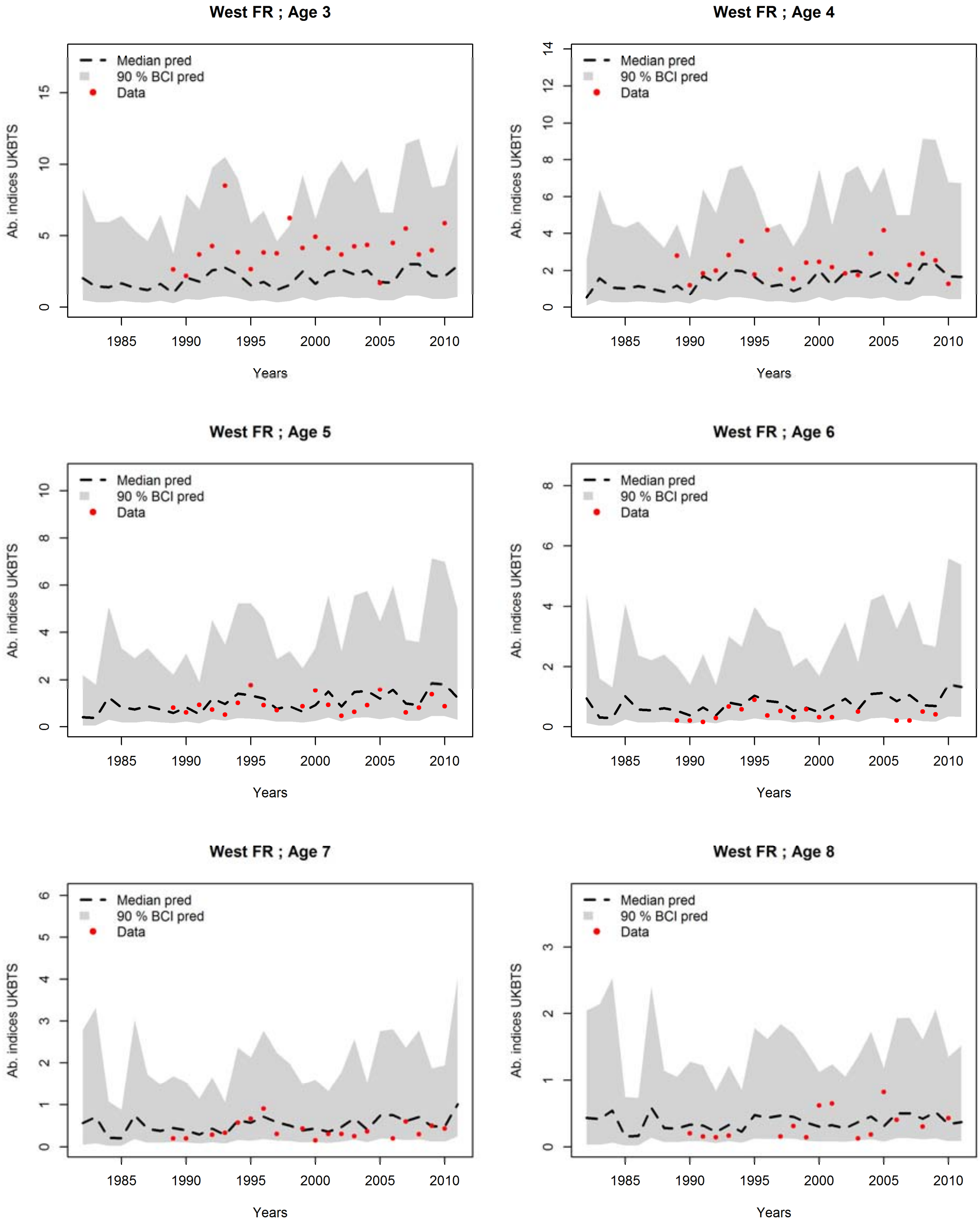

Fig. S2.7. Posterior predictive distribution and observations for the spatial scientific abundance indices in the West FR area (age-3 to age-8). Dots : Observations; Dotted lines: medians of the posterior predictive distribution; Shaded areas: 90% Bayesian credible intervals for the posterior predictive distribution.

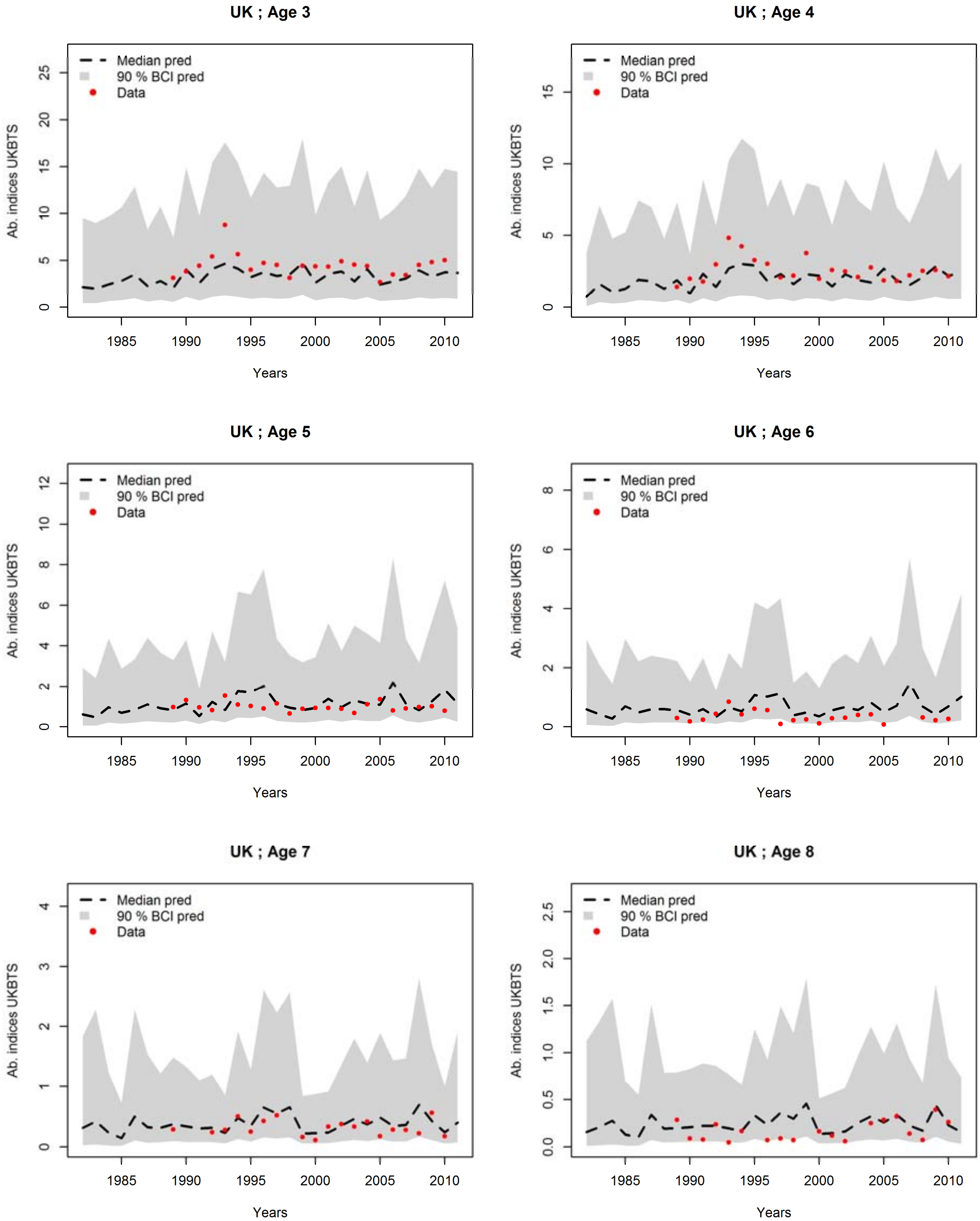

Fig. S2.8. Posterior predictive distribution and observations for the spatial scientific abundance indices in the UK area (age-3 to age-8). Dots : Observations; Dotted lines: medians of the posterior predictive distribution; Shaded areas: 90% Bayesian credible intervals for the posterior predictive distribution.

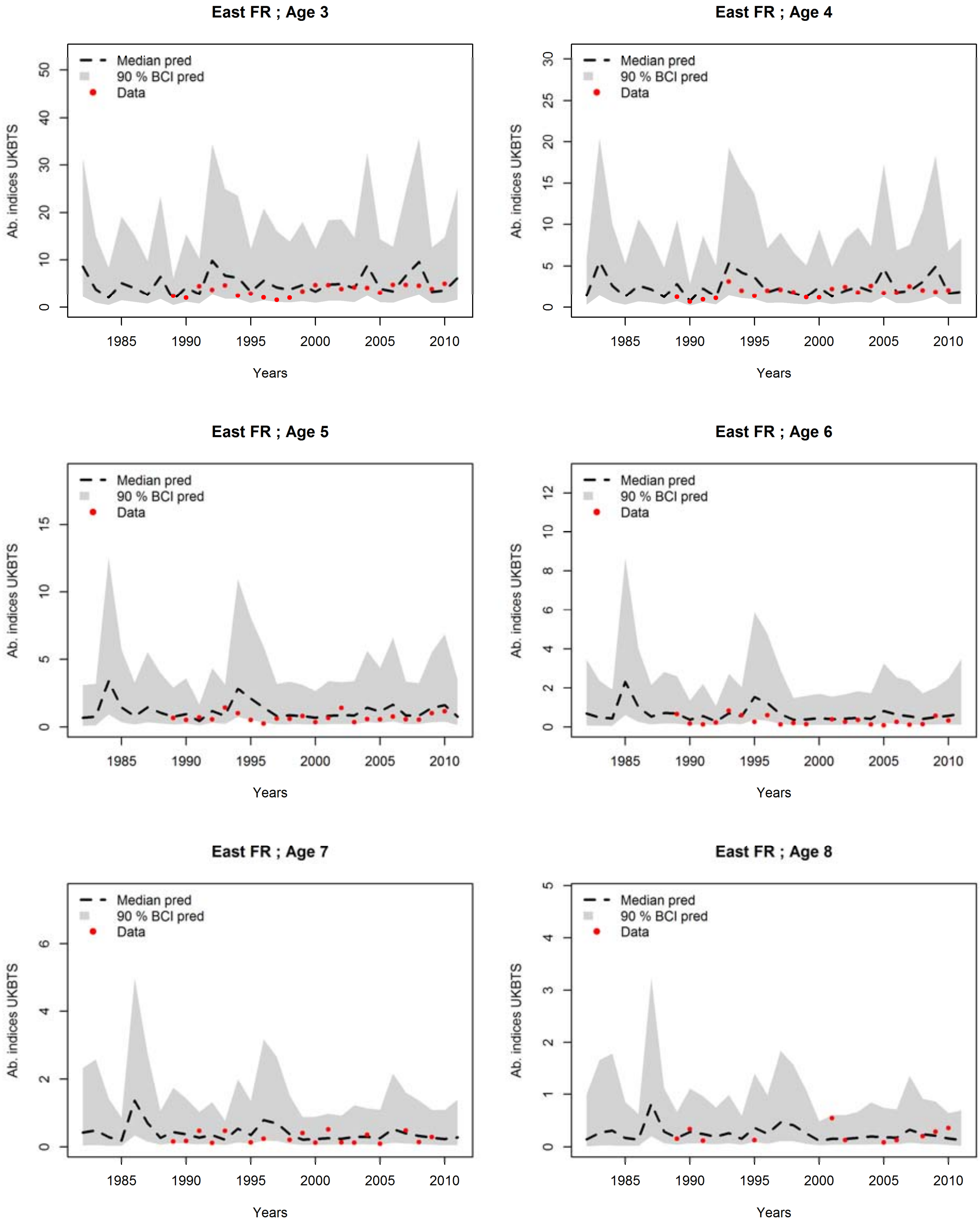

Fig. S2.9. Posterior predictive distribution and observations for the spatial scientific abundance indices in the East FR area (age-3 to age-8). Dots : Observations; Dotted lines: medians of the posterior predictive distribution; Shaded areas: 90% Bayesian credible intervals for the posterior predictive distribution.

Supplementary Material S3

Posterior distributions of estimated parameters for the model considering one single populations and the model considering three subpopulations.

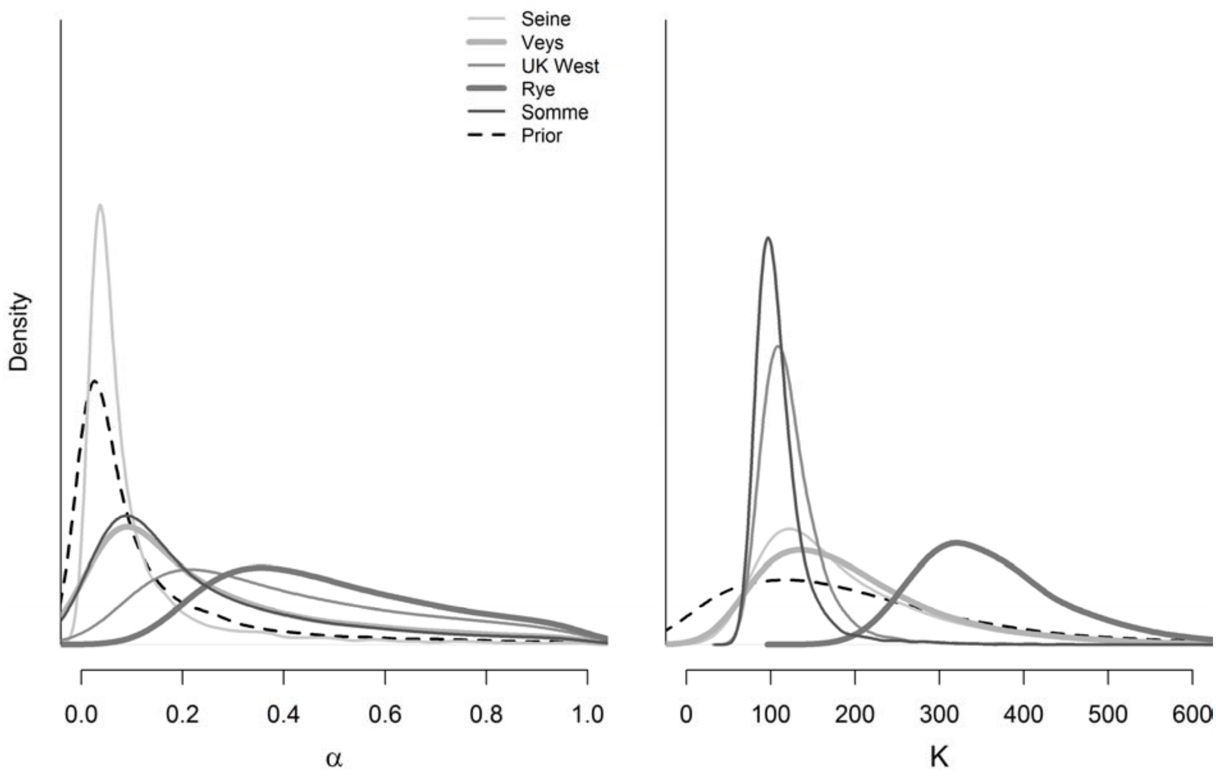

Fig. S3.1. Prior and marginal posterior distributions of the parameters α_i's and K_i's (in log-scale) for the five nursery sectors obtained with the model considering one single homogeneous population. The prior distributions on the α_i's is informative (See Appendix A). The prior distribution on the K_i's is weakly informative. An additional constraint $(\alpha < 1)$ is introduced in the model ($\alpha > 1$ would mean more 0+ juveniles than settled larvae).

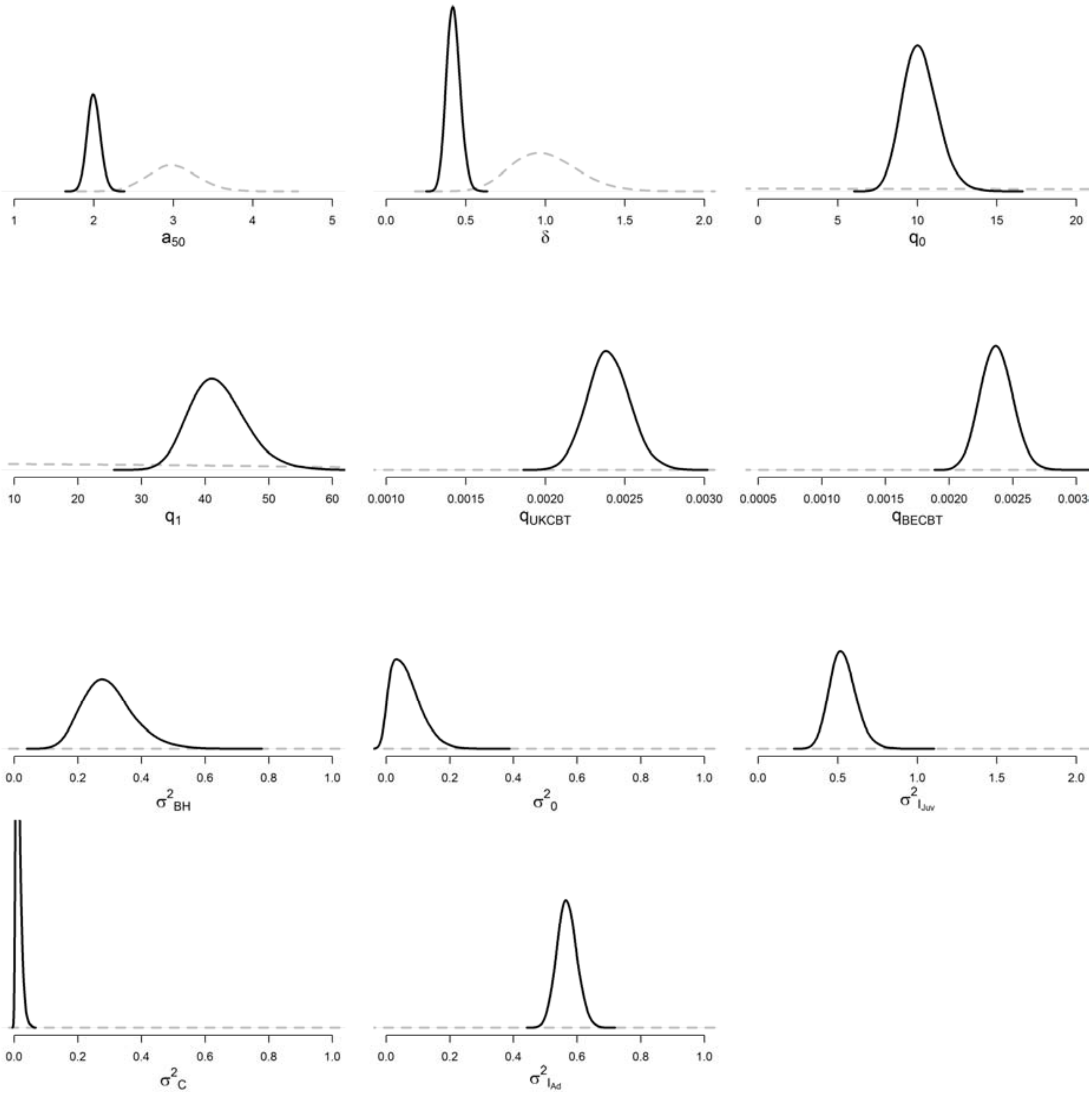

Fig. S3.2 Prior and marginal posterior distributions of all parameters obtained with the model considering one single homogeneous population. Dotted gray line: prior; Solid black line: posterior.

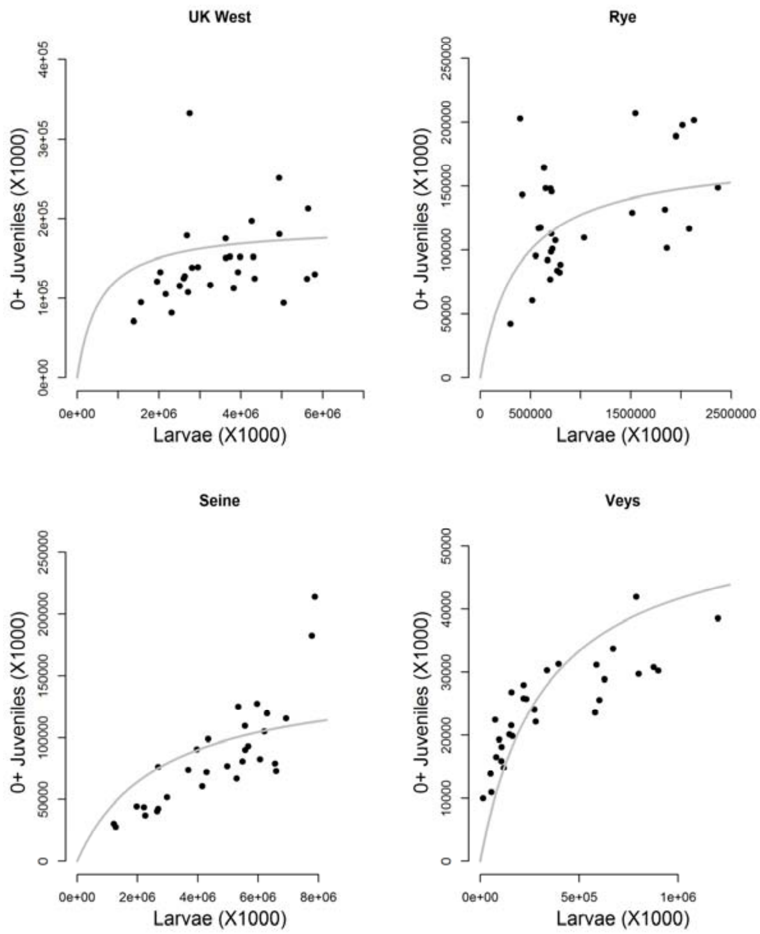

Fig. S3.3. Fit of the Beverton-Holt recruitment curve in each nursery sectors obtained with the model considering one single homogeneous population. Plain line: Bev-Holt curve drawn with the posterior medians of the (α, K) parameters. Black points: posterior medians of the number of larvae (x-axis) and age-0 juveniles (y-axis).

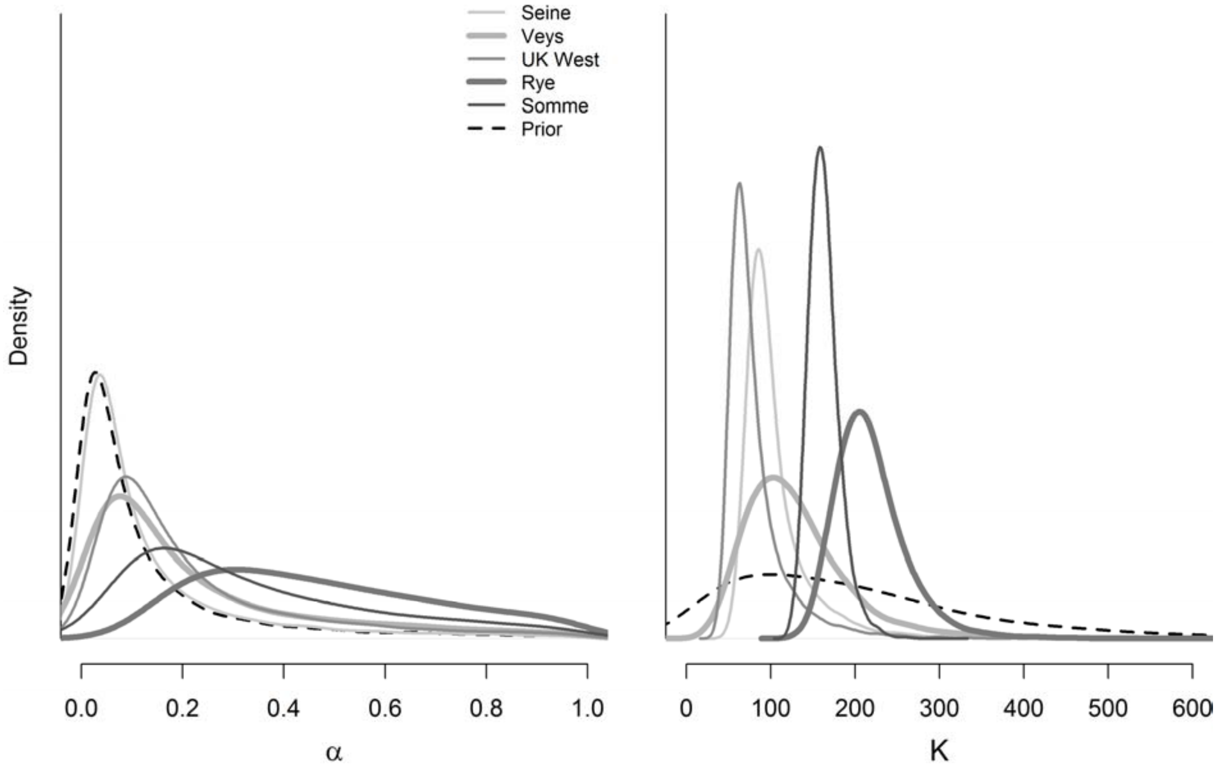

Fig. S3.4. Prior and marginal posterior distributions of the parameters α_i's and K_i's (in log-scale) for the five nursery sectors obtained with the model considering three subpopulations. The prior distributions on the α_i's is informative (See Appendix A). The prior distribution on the K_i's is weakly informative. An additional constraint ($\alpha < 1$) is introduced in the model ($\alpha > 1$ would mean more 0+ juveniles than settled larvae).

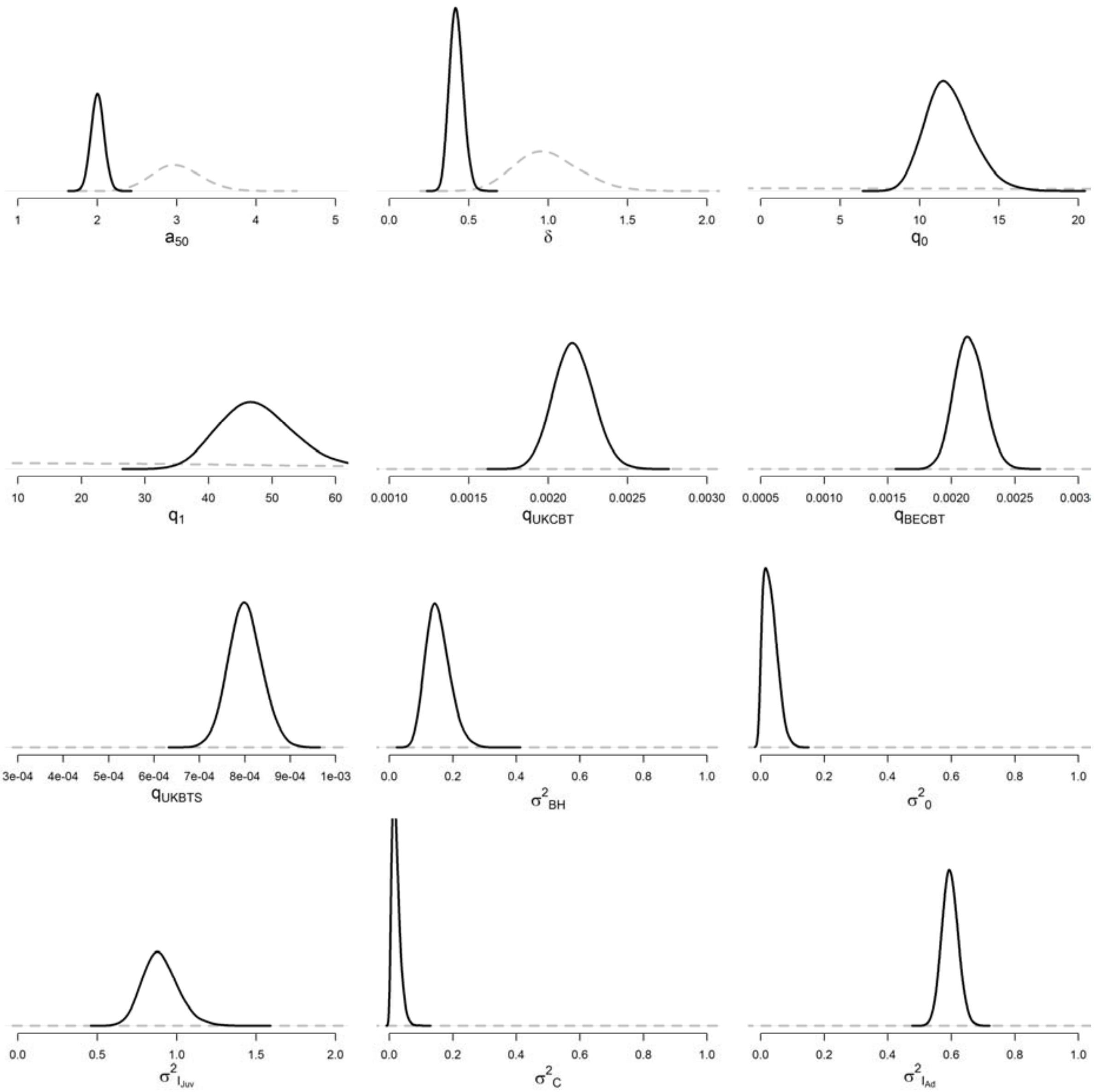

Fig. S3.5. Prior and marginal posterior distributions of all parameters obtained with the model considering three subpopulations. Dotted gray line: prior; Solid black line: posterior.

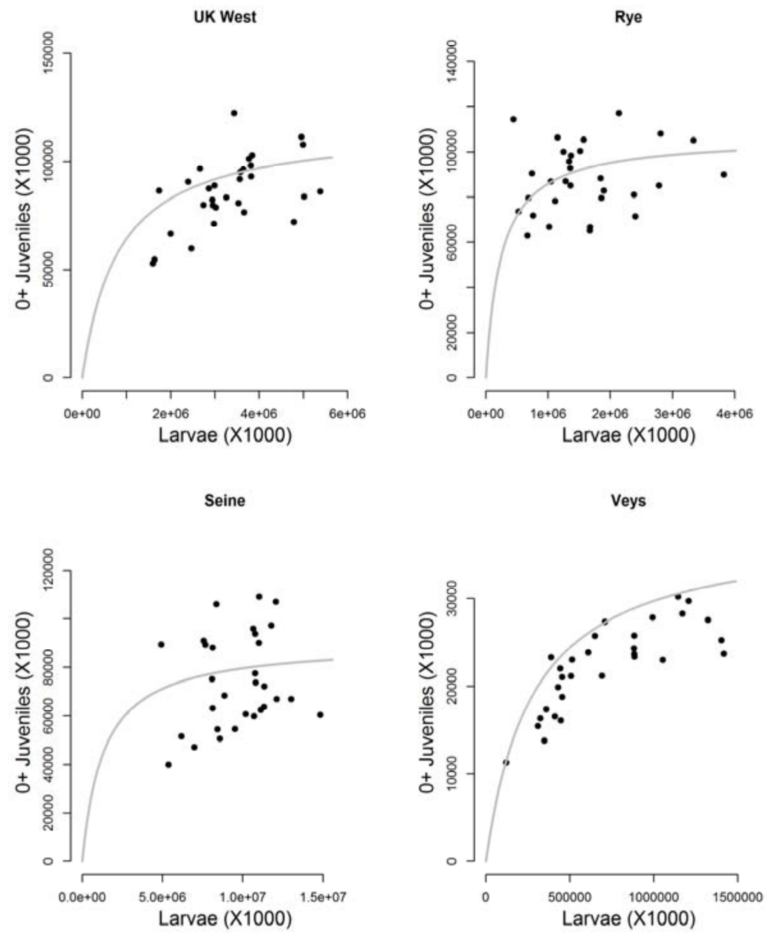

Fig. S3.6. Fit of the Beverton-Holt recruitment curve in each nursery sectors obtained with the model considering three subpopulations. Plain line: Bev-Holt curve drawn with the posterior medians of the (α, K) parameters. Black points: posterior medians of the number of larvae (x-axis) and age-0 juveniles (y-axis).

Tab. S3.1. Mean, median, standard deviation (sd) and quantiles 10 and 90% for marginal posterior distributions of parameters in the model considering one single homogeneous population.

Parameters	Mean	Median	Sd	q10	q90
α_1	0.41	0.35	0.24	0.13	0.78
α_2	0.5	0.46	0.21	0.25	0.83
α_3	0.24	0.16	0.22	0.044	0.58
α_4	0.11	0.056	0.15	0.024	0.25
α_5	0.25	0.17	0.23	0.041	0.61
K_1	120	120	39	87	170
K_2	370	350	96	260	490
K_3	110	100	38	82	140
K_4	190	160	110	89	330
K_5	200	170	110	86	340
a_{50}	2	2	0.034	1.9	2
δ	0.44	0.44	0.019	0.41	0.46
σ^2_{BH}	0.3	0.29	0.078	0.2	0.4
σ^2_0	0.064	0.056	0.046	0.012	0.13
σ^2_C	0.013	0.012	0.0083	0.0048	0.025
$\sigma^2_{I_{juv}}$	0.53	0.53	0.082	0.44	0.64
$\sigma^2_{I_{Ad}}$	0.57	0.57	0.03	0.53	0.61
q_0	10	10	1.1	8.9	12
q_1	42	42	4.4	37	48
q_{BECBT}	0.0024	0.0024	0.00012	0.0022	0.0025
q_{UKCBT}	0.0024	0.0024	0.00013	0.0022	0.0026

Tab. S3.2. Mean, median, standard deviation (sd) and quantiles 10 and 90% for marginal posterior distributions of parameters in the model considering three subpopulations.

Parameters	Mean	Median	Sd	q10	q90
α_1	0.22	0.14	0.2	0.051	0.53
α_2	0.48	0.44	0.23	0.2	0.82
α_3	0.34	0.27	0.24	0.096	0.72
α_4	0.14	0.068	0.18	0.017	0.37
α_5	0.22	0.14	0.22	0.034	0.56
K_1	82	71	39	53	120
K_2	220	210	43	170	270
K_3	160	160	19	140	190
K_4	110	93	47	72	150
K_5	130	120	65	66	210
a_{50}	2	2	0.026	1.9	2
δ	0.4	0.4	0.014	0.38	0.42
σ^2_{BH}	0.15	0.15	0.037	0.11	0.2
σ^2_0	0.031	0.027	0.021	0.0054	0.06
σ^2_C	0.021	0.019	0.013	0.0073	0.038
$\sigma^2_{I_{juv}}$	0.9	0.89	0.11	0.77	1
$\sigma^2_{I_{Ad}}$	0.6	0.59	0.025	0.56	0.63
q_0	12	12	1.5	10	14
q_1	48	47	5.9	41	56
q_{BECBT}	0.0021	0.0021	0.00011	0.002	0.0023
q_{UKCBT}	0.0022	0.0022	0.00012	0.002	0.0023
q_{UKBTS}	0.0008	0.0008	0.000036	0.00076	0.00085

Tab. S3.3. Correlation matrix (joint posterior distribution) for parameters in the model considering one single homogeneous population.

Param.	α_1	α_2	α_3	α_4	α_5	K_1	K_2	K_3	K_4	K_5	a_{50}	δ	q_0	q_1	q_{BECBT}	q_{UKCBT}	σ^2_{BH}	σ^2_0	$\sigma^2_{I_{juv}}$	σ^2_C	$\sigma^2_{I_{Ad}}$
α_1		0.06	0	0.03	0.05	-0.46	-0.06	-0.04	-0.02	-0.04	0.01	0.01	-0.01	-0.02	-0.01	0.00	-0.02	0.00	-0.01	0.00	-0.02
α_2	0.06		0	0.03	0.05	-0.06	-0.49	-0.02	-0.07	-0.09	-0.01	-0.01	-0.05	-0.05	-0.01	-0.01	0.04	-0.01	0.02	0.01	0.00
α_3	0.05	0.05		0.03	0.05	-0.05	-0.02	-0.35	-0.01	-0.04	-0.01	-0.01	-0.03	-0.03	0.00	0.01	-0.01	0.00	0.00	0.01	0.01
α_4	0.03	0.03	0		0.04	-0.01	0.00	0.02	-0.43	-0.04	0.00	-0.01	-0.03	-0.01	0.00	-0.01	0.12	0.07	0.02	0.01	-0.01
α_5	0.05	0.05	0	0.04		-0.04	-0.08	-0.04	-0.05	-0.21	-0.01	-0.01	0.04	0.07	-0.02	-0.02	0.03	0.00	0.01	0.00	0.00
K_1	-0.46	-0.06	-	-0.01	-0.04		0.00	0.02	-0.04	0.00	0.02	0.02	0.05	0.06	0.01	-0.02	0.09	-0.04	0.04	0.00	0.01
K_2	-0.06	-0.49	-	0.00	-0.08	0.00		0.01	0.08	0.10	0.01	0.00	-0.11	-0.08	-0.01	-0.01	0.06	0.12	-0.07	0.02	-0.01
K_3	-0.04	-0.02	-	0.02	-0.04	0.02	0.01		-0.02	0.00	0.01	0.01	-0.06	-0.04	-0.01	-0.02	0.10	0.05	-0.01	0.01	0.02
K_4	-0.02	-0.07	-	-0.43	-0.05	-0.04	0.08	-0.02		0.04	0.01	0.01	0.02	0.01	-0.01	0.01	-0.12	-0.06	-0.02	0.00	-0.01
K_5	-0.04	-0.09	-	-0.04	-0.21	0.00	0.10	0.00	0.04		0.01	0.01	0.04	0.08	0.00	0.00	0.03	0.03	-0.02	-0.01	-0.01
a_{50}	0.01	-0.01	-	0.00	-0.01	0.02	0.01	0.01	0.01	0.01		0.71	0.00	-0.01	0.27	0.25	0.02	-0.01	0.00	0.04	0.02
δ	0.01	-0.01	-	-0.01	-0.01	0.02	0.00	0.01	0.01	0.01	0.71		0.01	-0.01	0.15	0.15	0.01	-0.02	-0.01	-0.07	0.01
q_0	-0.01	-0.05	-	-0.03	0.04	0.05	-0.11	-0.06	0.02	0.04	0.00	0.01		0.33	0.05	0.05	0.06	-0.21	0.39	-0.07	0.01
q_1	-0.02	-0.05	-	-0.01	0.07	0.06	-0.08	-0.04	0.01	0.08	-0.01	-0.01	0.33		0.04	0.05	0.04	-0.01	0.36	-0.05	-0.01
q_{BECBT}	-0.01	-0.01	0	0.00	-0.02	0.01	-0.01	-0.01	-0.01	0.00	0.27	0.15	0.05	0.04		0.46	0.01	0.01	-0.01	-0.08	0.32
q_{UKCBT}	0.00	-0.01	0	-0.01	-0.02	-0.02	-0.01	-0.02	0.01	0.00	0.25	0.15	0.05	0.05	0.46		0.01	0.00	-0.01	-0.06	0.29
σ^2_{BH}	-0.02	0.04	-	0.12	0.03	0.09	0.06	0.10	-0.12	0.03	0.02	0.01	0.06	0.04	0.01	0.01		0.07	-0.19	-0.01	0.00
σ^2_0	0.00	-0.01	0	0.07	0.00	-0.04	0.12	0.05	-0.06	0.03	-0.01	-0.02	-0.21	-0.01	0.01	0.00	0.07		-0.24	-0.01	0.00
$\sigma^2_{I_{juv}}$	-0.01	0.02	0	0.02	0.01	0.04	-0.07	-0.01	-0.02	-0.02	0.00	-0.01	0.39	0.36	-0.01	-0.01	-0.19	-0.24		0.00	-0.02
σ^2_C	0.00	0.01	0	0.01	0.00	0.00	0.02	0.01	0.00	-0.01	0.04	-0.07	-0.07	-0.05	-0.08	-0.06	-0.01	-0.01	0.00		-0.02
$\sigma^2_{I_{Ad}}$	-0.02	0.00	0	-0.01	0.00	0.01	-0.01	0.02	-0.01	-0.01	0.02	0.01	0.01	-0.01	0.32	0.29	0.00	0.00	-0.02	-0.02	

Tab. S3.4. Correlation matrix (joint posterior distribution) for parameters of parameters in the model considering three subpopulations.

Param.	α_1	α_2	α_3	α_4	α_5	K_1	K_2	K_3	K_4	K_5	a_{50}	δ	q_0	q_1	q_{BECBT}	q_{UKBTS}	q_{UKCBT}	σ^2_{BH}	σ^2_0	$\sigma^2_{I_{juv}}$	σ^2_C	$\sigma^2_{I_{Ad}}$
α_1		0.02	0	0.03	0.07	-0.45	-0.04	-0.04	0.01	-0.02	0.00	0.00	-0.01	-0.01	0.00	0.01	-0.01	0.00	0.00	-0.02	0.01	0.00
α_2	0.02		0	0.03	0.08	-0.02	-0.46	-0.08	0.00	-0.05	0.01	-0.01	-0.03	-0.02	-0.01	0.00	0.00	-0.05	0.02	0.01	0.01	-0.01
α_3	0.04	0.11		0.03	0.05	-0.03	-0.10	-0.38	0.02	-0.02	0.00	-0.01	-0.01	-0.01	0.00	0.02	-0.01	-0.07	-0.02	0.00	0.02	0.01
α_4	0.02	0.03	0		-0.02	-0.04	-0.01	0.01	-0.35	-0.05	-0.01	0.00	0.00	-0.01	0.00	0.01	0.02	0.02	0.01	0.01	-0.01	0.02
α_5	0.07	0.08	0	-0.02		-0.04	-0.07	-0.05	-0.03	-0.29	0.01	-0.01	0.01	0.03	0.02	0.01	0.01	0.04	0.01	-0.04	0.02	0.00
K_1	-0.45	-0.02	-	-0.04	-0.04		-0.06	0.04	0.04	0.05	0.01	0.00	0.00	0.02	0.00	-0.02	0.00	0.06	-0.01	0.01	0.01	0.01
K_2	-0.04	-0.46	-	-0.01	-0.07	-0.06		0.10	0.00	0.08	0.01	0.01	-0.08	-0.07	-0.02	-0.02	-0.02	0.08	0.06	-0.05	0.03	0.00
K_3	-0.04	-0.08	-	0.01	-0.05	0.04	0.10		-0.01	0.03	0.03	0.00	-0.02	0.00	-0.06	-0.05	-0.05	0.15	-0.02	0.04	0.03	-0.02
K_4	0.01	0.00	0	-0.35	-0.03	0.04	0.00	-0.01		-0.01	0.01	0.01	-0.03	-0.01	0.00	-0.02	-0.02	-0.05	-0.01	0.00	0.02	-0.01
K_5	-0.02	-0.05	-	-0.05	-0.29	0.05	0.08	0.03	-0.01		0.01	0.00	-0.01	0.02	-0.01	-0.01	-0.01	0.01	0.01	-0.01	0.01	0.01
a_{50}	0.00	0.01	0	-0.01	0.01	0.01	0.01	0.03	0.01	0.01		0.66	0.00	0.00	0.25	0.31	0.24	0.02	0.00	0.02	-0.02	0.02
δ	0.00	-0.01	-	0.00	-0.01	0.00	0.01	0.00	0.01	0.00	0.66		0.00	0.00	0.17	0.22	0.16	0.04	0.01	0.00	-0.15	0.00
q_0	-0.01	-0.03	-	0.00	0.01	0.00	-0.08	-0.02	-0.03	-0.01	0.00	0.00		0.27	0.01	0.05	0.04	0.04	-0.04	0.47	-0.07	0.00
q_1	-0.01	-0.02	-	-0.01	0.03	0.02	-0.07	0.00	-0.01	0.02	0.00	0.00	0.27		0.03	0.04	0.05	0.03	0.01	0.45	-0.07	0.01
q_{BECBT}	0.00	-0.01	0	0.00	0.02	0.00	-0.02	-0.06	0.00	-0.01	0.25	0.17	0.01	0.03		0.41	0.48	0.03	0.01	-0.02	-0.16	0.26
q_{UKBTS}	0.01	0.00	0	0.01	0.01	-0.02	-0.02	-0.05	-0.02	-0.01	0.31	0.22	0.05	0.04	0.41		0.41	0.05	0.02	-0.01	-0.20	0.32
q_{UKCBT}	-0.01	0.00	-	0.02	0.01	0.00	-0.02	-0.05	-0.02	-0.01	0.24	0.16	0.04	0.05	0.48	0.41		0.03	0.00	0.01	-0.14	0.24
σ^2_{BH}	0.00	-0.05	-	0.02	0.04	0.06	0.08	0.15	-0.05	0.01	0.02	0.04	0.04	0.03	0.03	0.05	0.03		-0.19	-0.04	-0.18	0.02
σ^2_0	0.00	0.02	-	0.01	0.01	-0.01	0.06	-0.02	-0.01	0.01	0.00	0.01	-0.04	0.01	0.01	0.02	0.00	-0.19		-0.03	-0.07	0.02
$\sigma^2_{I_{juv}}$	-0.02	0.01	0	0.01	-0.04	0.01	-0.05	0.04	0.00	-0.01	0.02	0.00	0.47	0.45	-0.02	-0.01	0.01	-0.04	-0.03		-0.01	0.00
σ^2_C	0.01	0.01	0	-0.01	0.02	0.01	0.03	0.03	0.02	0.01	-0.02	-0.15	-0.07	-0.07	-0.16	-0.20	-0.14	-0.18	-0.07	-0.01		-0.04
$\sigma^2_{I_{Ad}}$	0.00	-0.01	0	0.02	0.00	0.01	0.00	-0.02	-0.01	0.01	0.02	0.00	0.00	0.01	0.26	0.32	0.24	0.02	0.02	0.00	-0.04	